rivm

National Institute
for Public Health
and the Environment

Report 680150003/2008

A.J.C. Berkhout et al.

Measuring ammonia emissions from manured fields

ECN

WAGENINGEN UNIVERSITY
WAGENINGEN UR

rivm

RIVM Report 680150003/2008

Measuring ammonia emissions from manured fields

A.J.C. Berkhout, RIVM
G.R. van der Hoff, RIVM
J.B. Bergwerff, RIVM
D.P.J. Swart, RIVM
A. Hensen, ECN
A. Kraai, ECN
A. Bleeker, ECN
J.F.M. Huijsmans, WUR
J. Mosquera, WUR
W.A.J. van Pul, RIVM

Contact:
W.A.J. van Pul
Laboratory for Environmental Monitoring
addo.van.pul@rivm.nl

This investigation has been performed by order and for the account of the Ministry of VROM, within the framework of project M/680150/Ammonia.

rivm

Abstract

Measuring ammonia emissions from manured fields

The Dutch National Institute for Public Health and the Environment (RIVM)and the Energy Research Centre of the Netherlands (ECN) have developed two novel instruments to measure atmospheric ammonia emissions from manured fields – a lidar (light detection and ranging) and a TDL (tuneable diode laser). Insight into ammonia emissions is necessary in order to comply with European Union policy that current emission levels be reduced by 2010. Ammonia causes the eutrophication and acidification of nature reserves and contributes to the formation of particulate matter.

The measurements obtained using the lidar and TDL are in good agreement. On grassland, both instruments measured relatively high levels of emissions relative to those obtained in the past using other instruments, but the values fell within the range of those past measurements. On arable land, the measurements obtained using the new methods did not differ from average emission levels based on previous measurements.

The new instruments revealed that ammonia emissions from a manured field peak later than expected: not directly after the manure is applied, but 1–2 hours later. Consequently, with the aim to improve national emission numbers, the use of a model that explicitly takes into account the most important environmental variables is recommended.

Key words:

ammonia, manure, slurry, emission, lidar, TDL, nitrogen

Rapport in het kort

Het meten van ammoniakemissies van bemeste velden

Het RIVM en het Energie Onderzoekcentrum Nederland (ECN) hebben twee nieuwe meetinstrumenten ontwikkeld om de ammoniakuitstoot van bemeste velden te meten. Het gaat om respectievelijk een LIDAR (Light Detection and Ranging) en een TDL (Tuneable Diode Laser). Een belangrijke reden om een goed beeld van ammoniakemissies te krijgen is de Europese verplichting om deze emissies voor 2010 terug te dringen. Door ammoniak verzuren natuurgebieden en bevatten ze te veel voedingsstoffen. Ook draagt ammoniak bij aan de vorming van fijn stof.

De resultaten van de twee instrumenten komen goed met elkaar overeen. Op grasland meten ze relatief hoge emissies vergeleken bij metingen in het verleden, maar wel binnen de bandbreedte ervan. Op bouwland is geen verschil gemeten tussen de emissies met de nieuwe meetmethoden en gemiddelde emissies gebaseerd op eerdere metingen.

Daarnaast bleek de maximale uitstoot van een bemest veld op een ander moment op te treden dan verwacht: niet direct na het opbrengen van de mest, maar een tot twee uur later. Om de nationale emissiecijfers te verbeteren verdient het daarom aanbeveling een rekenmodel te gebruiken dat expliciet de belangrijkste omgevingsfactoren meeneemt.

Trefwoorden:

ammoniak, mest, emissie, LIDAR, TDL, stikstof

Acknowledgement

The authors wish to thank the organisations and persons who made available their grounds or farms for this research: Nissan in Amsterdam, the Oostwaardhoeve in Slootdorp, and the Kastelijn-Hol family in Kamerik.

rivm

Contents

Summary		**11**
1	**Introduction**	**13**
1.1	Measuring ammonia emissions	13
1.1.1	Measurement techniques	13
1.1.2	Emission measurement experiments	14
1.2	Report overview	14
2	**Methods**	**15**
2.1	ECN – mobile TDL spectrometers and a stationary monitor	15
2.1.1	Concentration measurements	15
2.1.2	Meteorological data	17
2.1.3	Emission calculation	17
2.2	RIVM – mobile lidar	20
2.2.1	Concentration measurements	20
2.2.2	Meteorological data	24
2.2.3	Emission calculation	25
2.3	WUR – micrometeorological mass balance method	26
2.3.1	Concentration measurements	26
2.3.2	Meteorological data	27
2.3.3	Emission calculation	28
2.4	Emission measurements experimental set-up	30
2.5	Manure analysis	31
3	**Results and discussion**	**33**
3.1	Measurement locations	33
3.2	Artificial ammonia source – Amsterdam, 9 August 2006	34
3.2.1	Experimental set-up	34
3.2.2	Measurement results	36
3.2.3	Discussion	39
3.3	Manured field section 1 – Oostwaardhoeve, 18-19 October 2006	40
3.3.1	Experimental set-up	40
3.3.2	Measurement results	42
3.3.3	Discussion	45
3.4	Manured field section 2 – Oostwaardhoeve, 14-17 March 2007	46
3.4.1	Experimental set-up	46
3.4.2	Measurement results	48
3.4.3	Discussion	51
3.5	Manured field – Oostwaardhoeve, 27 March 2007	52
3.5.1	Experimental set-up	52
3.5.2	Measurement results	55
3.5.3	Discussion	58
3.6	Manured field 1 – Woerden, 3 August 2007	59
3.6.1	Experimental set-up	59
3.6.2	Measurement results	63

3.6.3	Discussion	66
3.7	Manured field 2 – Woerden, 10 August 2007	67
3.7.1	Experimental set-up	67
3.7.2	Measurement results	68
3.7.3	Discussion	69
3.8	Manured field 3 – Woerden, 13 August 2007	70
3.8.1	Experimental set-up	70
3.8.2	Measurement results	71
3.8.3	Discussion	73
3.9	General discussion	73
4	**Conclusions**	**75**
4.1	Recommendations	75
References		**77**
Appendix		**79**

rivm

Summary

The ammonia emission after manure application is still an uncertain factor in the Dutch national ammonia emission budget. The bulk of the emission occurs in the first hours after manure application. The emissions associated with different application techniques were evaluated in the past on experimental plots, but little information is available on emissions from entire fields. In this report, two novel instruments are described that are able to measure the ammonia emissions of manured fields.

The first instrument, developed and operated by ECN, is a tuneable diode laser spectrometer (TDL), mounted in a van. It is used to measure the ammonia concentration patterns downwind from a manured field. Wind measurements, a nitrous oxide tracer and a simple Gaussian plume model are used to calculate the ammonia emission.

The second instrument, built by RIVM, is a mobile lidar system. It measures a two-dimensional ammonia concentration profile, also downwind from a manured field. This is combined with wind measurements to compute the ammonia emission.

The new instruments were applied to measure ammonia emissions from manured fields in six field experiments (the TDL in four), three on arable land and three on grassland. For the four experiments in which both instruments had been present, the results were compared to each other. Additionally, in one of the experiments, both instruments were compared to the micrometeorological mass balance method, an established technique. In all experiments, the agreement between the emission patterns found by all different methods was good.

In all experiments described in this report, the measured emission rates peaked around one or two hours after the end of the manure application. Lidar and TDL were able to see this effect because their temporal resolution was high as compared to the mass balance method.

Two of the experiments spanned two days. In both cases, a significant emission was found on the second day after the manure had been applied. This emission amounted to 25% of the emission measured during the first day.

The measured emissions were also compared to measurements performed in the past. On arable land, the results of the current experiments fit within the range of the results of the past experiments. On grassland, the emissions found in these experiments were relatively high, but within the range found in experiments performed in the past.

It is recommended to have future experiments take place on grassland. The established micrometeorological mass balance method should be included. Those experiments should provide additional insight in the dynamics of the emission process. The TDL and lidar methods, with their high temporal resolution, are especially suited for such research. It is also recommended to model the process of ammonia emission, and to integrate this model with a statistical model of field measurements of ammonia losses.

1 Introduction

The emissions of ammonia after manure application form a relatively large part of the ammonia emissions in the Netherlands. In 2007, 32% of the ammonia emissions is estimated to originate from manure spreading (Milieu- en Natuurcompendium 2008). The emissions after manure spreading decreased considerably over the last two decades because of the reduction techniques that have been obligatory since 1989.

Evaluation of the national ammonia emissions is carried out in the Netherlands by calculating the ammonia concentration with an atmospheric transport model using the emissions. The calculated concentrations are subsequently compared to measured ammonia concentrations. From this comparison it is clear that the measured concentrations are underestimated by the model by about 30% (Van Pul et al. 2004). The discrepancy is mainly caused by uncertainties in the model calculations on one hand and uncertainties in the emissions on the other hand.

Considering the emissions, some doubt exists about the effectiveness of the reduction techniques which are used by manure application. Recently, it was found from the VELD-project in the Netherlands that the emissions during springtime were greatly underestimated (Smits et al. 2005). Activities were initiated to get insight in the reasons for this underestimation, both in the field of the emission factors as well as in agricultural practice.

The emission of ammonia from fields is a process that is dependent on a large number of environmental and agricultural factors (Huijsmans 2003). This makes this evaporation process highly variable in time. The bulk of the emission occurs in the first hours after manure application. The emissions associated with different application techniques were evaluated in the past on experimental plots, but little information is available on emissions from entire fields. In this report, two novel measurement techniques are described that are able to measure the ammonia emissions of manured fields. Their application was performed in a joint project by ECN, RIVM and WUR, and entailed direct measurements of the emissions under field conditions.

1.1 Measuring ammonia emissions

1.1.1 Measurement techniques

The first novel measurement technique reported here, is a tuneable diode laser spectrometer (or TDL), operating in the IR (Hensen et al. 2008). This instrument is partly built and fully operated by ECN. It is combined with a wet chemical fast response denuder, for calibration purposes. The instrument is mounted in a van. It is used to measure the ammonia concentration patterns downwind from a manured field. Wind measurements, a nitrous oxide tracer and a simple Gaussian plume model are used to calculate the ammonia emission.

The second instrument, built and operated by RIVM, is a mobile lidar system. Lidar, short for light detection and ranging, is a technique similar to radar, and may be used to remotely measure the concentration of a trace gas in the atmosphere. The mobile lidar uses a UV laser to measure a two-

dimensional ammonia concentration profile, also downwind from a manured field. This is combined with wind measurements to compute the ammonia emission of the field.

The results from these new instruments were in one experiment compared to results obtained synchronously with the micrometeorological mass balance method. This method, operated in the campaign reported on here by WUR, is an established measurement technique (Denmead 1983; Huijsmans et al. 2001; Ryden and Mcneill 1984) to measure the emission of a circular manured plot. A mast supporting a number of ammonia traps at different heights is placed in the centre of the manured plot. These traps are replaced at regular intervals, and analysed in the laboratory for ammonium. From the concentration profile obtained, combined with a profile from a background mast and with synchronously measured meteorological parameters, the cumulative emission is calculated.

1.1.2 Emission measurement experiments

The TDL and lidar techniques were tested and operated in a short measurement campaign. This campaign encompassed experiments that were carried out at three different locations. The first experiment, carried out in Amsterdam, aimed at a comparison of the TDL and lidar measurement techniques using an artificial source with a known source distribution and source strength. The source strength was relatively constant over time. The experiment took place on an asphalted area, without vegetation and therefore with hardly any deposition.

At the Oostwaardhoeve, an experimental farm at Slootdorp, the first two experiments had a setup that was similar to the standard experimental setup for the micrometeorological mass balance method as described by Huijsmans et al. (Huijsmans 2003; Huijsmans et al. 2001). A manured circle was used as a source. The source strength was high at the start of the experiments and decreased over time as the ammonia evaporated. Also at the Oostwaardhoeve, a full-field manure application experiment was conducted. The experiment and its interpretation were completely different, as application of manure continued during the emission measurements. All three experiments at the Oostwaardhoeve took place on arable land.

An intermediate setup with a large manured area that was still small enough to be manured within a short period of time was tested at Woerden in three subsequent experiments. These were all conducted on grassland.

1.2 Report overview

Chapter 2 is devoted to the measurement methods. First the two novel methods, the TDL and the mobile lidar, are described, then the micrometeorological mass balance method. Finally, the measurement procedures on an experimental day are outlined.

In chapter 3, the results of all the experiments are reported and discussed. First, the experiment on the artificial ammonia source is described, then the three experiments on arable land at the Oostwaardhoeve, and finally the three experiments on grassland in Woerden.

The report finishes with conclusions (chapter 4) and recommendations for further research.

2 Methods

2.1 ECN – mobile TDL spectrometers and a stationary monitor

2.1.1 Concentration measurements

General set-up

Downwind of the NH_3 source a plume of NH_3 can be observed using a mobile Tuneable Diode Laser (TDL) spectrometer. The shape of this plume is determined both by the dimensions of the source and by meteorological circumstances.

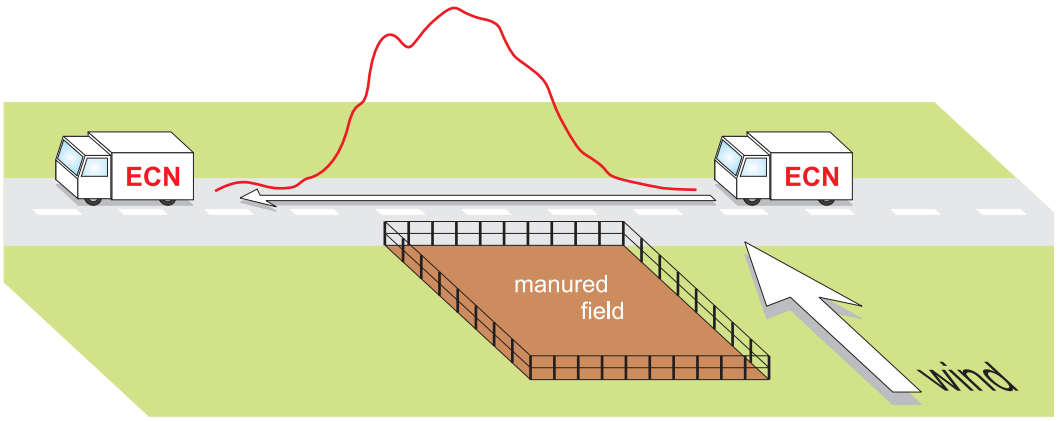

Figure 2-1. Scheme showing how the TDL is used to measure the ammonia emission of a manured field.

Concentrations of NH_3 from the field and of N_2O released from a gas flask release system were both measured using tuneable diode laser spectrometers. The latter is used to determine the parameters in the Gaussian dispersion model (see section 2.1.3 below), which is used to calculate the emissions from the concentration data.

NH_3 and N_2O concentration measurements

The TDL system (Aerodyne, Billerica USA) uses the 1010 cm^{-1} absorption line for NH_3 and a closed multi-pass cell (0.5 L, 50 Torr, 32 m path) to measure the concentration along a transect in the plume. The TDL was mounted in a van, air was sampled from the window adjacent to the instruments and lead to the measurement cell through a 1 m length, ¼ inch diameter polyethene tube. A high flow rate of about 20 L min^{-1} was used to minimise the storage effect of NH_3 on the inlet (see discussion below). Concentration measurements were done at 0.5 Hz. The system had a noise level of about 10% on the concentration measurements. With this set-up, concentration levels above the noise level of about 50 µg m^{-3} could be measured. An example of several plume measurements is shown in Figure 2-2.

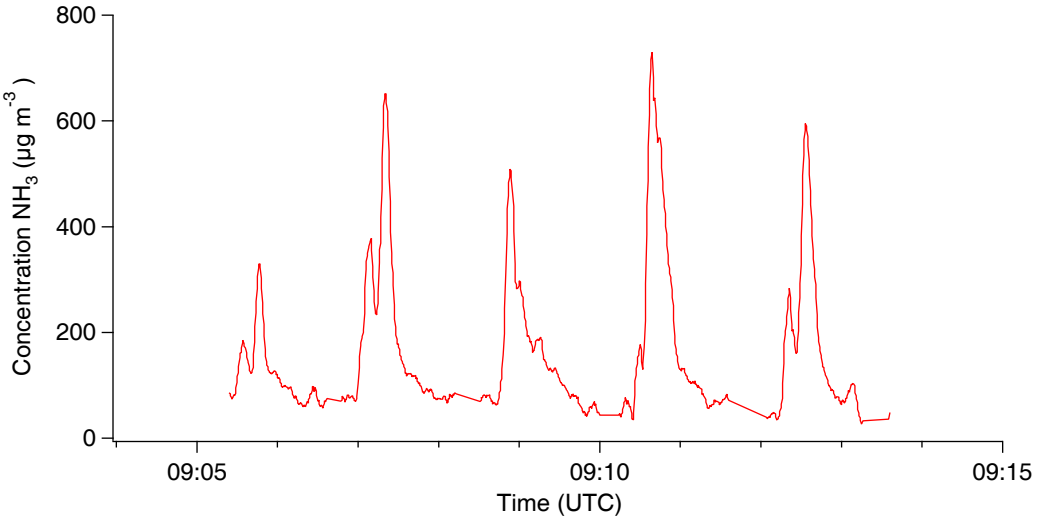

Figure 2-2. Example of five NH_3 plumes that were obtained during the experiment in Amsterdam, 9 August 2006. On this day the system had a noise level of about 20 µg m^{-3}, the concentration peaks were between 300 and 600 µg m^{-3}.

The N_2O TDL is identical in set-up to the NH_3 TDL, but uses the 2216 cm^{-1} line to evaluate the N_2O concentration.

Inlet configuration

Compared to N_2O, NH_3 is a very reactive gas which is easily lost in any sort of inlet system. At the first manure spreading experiment at the Oostwaardhoeve, experiments with a longer inlet line were performed. A reason to use a longer inlet line was to avoid disturbance of the plume by the car. However, as will be discussed below, the longer inlet line only caused a significant damping that probably lead to a significant underestimation of the emission. The disturbance of the plume shape by the car remained. When the plume from the N_2O tracer and the NH_3 plume are of similar shape, and the two TDL systems use the same inlet, this disturbance however will also show on the reference N_2O plumes. This way, the effect will be included in the correction that is applied.

Calibration

The N_2O measurements were calibrated using N_2O in N_2 / O_2 mixtures of 300 and 500 ppb that were applied to the TDL on a regular basis during the experiment.

For NH_3 the calibration corrects for the effect of changing sensitivity of the TDL system which is caused mainly by interference fringes, related to dust particles on the mirror in the multi-pass cell. These particles cannot be filtered out from the inlet flow because of the reactive properties of NH_3; it will attach to any inlet filter system.

The calibration of the TDL data was done by intercomparison of either gas bag samples (80 L bags with concentrations ranging between 100 and 400 µg m^{-3}) or air with a high NH_3 concentration from a bubbling system. The concentration in the gas bag or in the exhaust air from the bubbler was determined with reference monitors; an Airrmonia or an Amanda, both wet chemical denuder systems. These reference monitors were calibrated against chemical solutions.

Amsterdam (August 2006) and Oostwaardhoeve 1 (October 2006): in these experiments an Airrmonia was used. This instrument can be used on board of the van but has the disadvantage that the response time is in the order of fifteen minutes. This made an intercomparison of concentration data difficult. Gas bag samples with 200-300 µg m^{-3} were applied both to the TDL and to the Airrmonia. With these data the concentration measurement of the TDL was calibrated. This calibration procedure caused significant gaps in the data.

Oostwaardhoeve 2 and 3 (March 2007): in these experiments an Amanda was placed on a fixed position for calibration purposes. The Amanda has a rotating wet denuder which has a response time of about four minutes. This makes calibration experiments significantly easier. This system however cannot be used while driving. Calibration was done by co-locating the TDL and Amanda for a few minutes. At the third Oostwaardhoeve experiment the Amanda data could not be used and calibration factors were obtained from gasbag intercomparison measurements in the lab the day before the experiment.

Woerden 1 (3 August 2007): in this experiment a bubbler system was used to generate a constant air flow of 40 L min^{-1} with a high NH_3 concentration (about 400 µg m^{-3} added to the local concentration). This system was tested and found to give a reproducible concentration increase with a 10% uncertainty. The bubbler was used a number of times during the day at the TDL and checked twice at the Amanda.

2.1.2 Meteorological data

Meteorological data (wind speed and wind direction) were obtained using a Mierij MMW005 solid state wind sensor at 1.8 m. The meteorological data was transmitted to the mobile measurement system at 1 Hz using a radio modem. The position of the measurement van was logged at 1 Hz using a GPS (Garmin G76).

2.1.3 Emission calculation

The emission from the source is calculated using the following equation:

$$Q = Q_{model} \cdot \frac{\Sigma_{meas}}{\Sigma_{model}} \qquad \text{Equation 1}$$

Q is the source strength, Q_{model} the value used to run the Gaussian dispersion model (see below) and Σ the integral of the measured or modelled concentration along the measurement transect. An example of two plume transect measurements is shown in Figure 2-3.

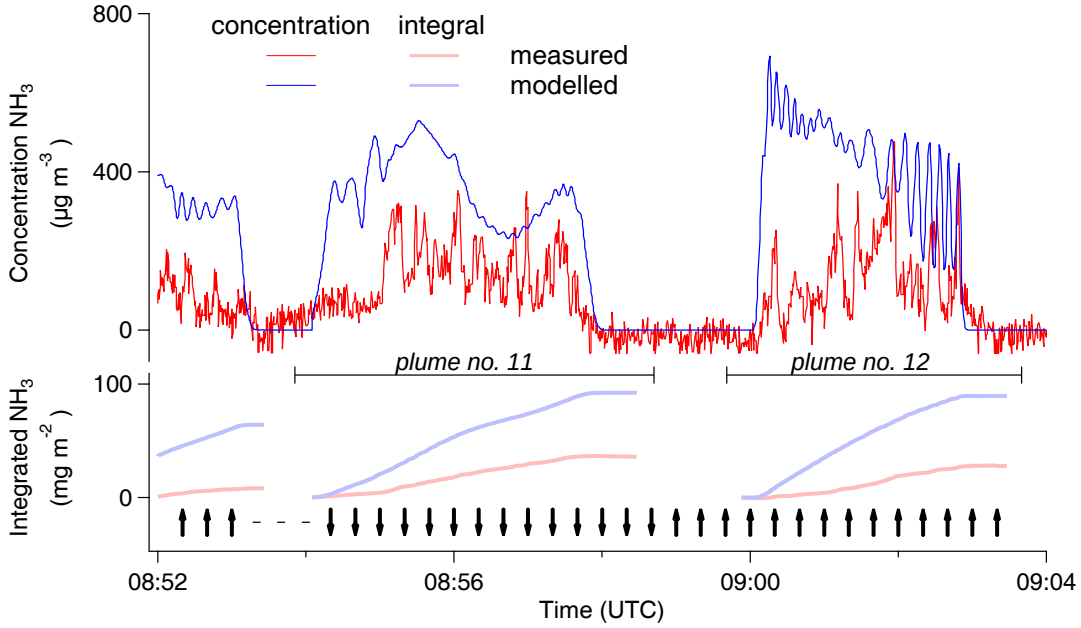

Figure 2-3. Woerden, 3 August 2007. The upper part of the graph shows the NH_3 concentrations along the plume transect, for plumes no. 11 (north to south) and 12 (south to north).

Red: measured concentrations, blue: modelled concentrations. The pale red and blue lines in the lower part of the graph are the integrated measured and modelled plumes; those are used to calculate the final emission estimate. The row of arrows at the bottom indicates the direction of the movement of the vehicle.

In Figure 2-3 example data obtained during the Woerden experiment of 3 August 2007 is shown. The comb-like pattern in the modelled concentration curve at 9:02 is no noise but occurs when the wind direction is aligned with the grid of point sources, causing the plumes to overlap. The set of peaks in the N_2O concentration curve at 8:53 are gas bag calibrations for N_2O. The lower half of the Figure shows the cumulative curves that represent the integral values, starting at the onset of the plumes and reaching their maximum when the plumes end. The ratio of the maximum levels of the two integrals (pale red and pale blue curves) is calculated from the maximum values of these two curves.

Gaussian dispersion model

In general the concentration downwind of a point source located at (x_s ,y_s, z_s) to a point receptor located at (x, y, z) can be described with the Gaussian plume equation, which was calculated using $X = x - x_s$ and $Y = y - y_s$, as:

$$C(X,Y,z) = \frac{Q}{2\pi \cdot \sigma_y \cdot \sigma_z} \cdot e^{-Y^2/(2\cdot\sigma_y)^2} \cdot \left(e^{-(z-h_s)^2/(2\cdot\sigma_z)^2} + e^{-(z+h_s)^2/(2\cdot\sigma_z)^2} \right) \quad \text{Equation 2}$$

$$\sigma_y = a \cdot X^b \cdot z_o^{0.2} \cdot T^{0.35} \quad \text{Equation 3}$$

$$\sigma_z = c \cdot X^d \cdot (10 \cdot z_o)^{0.53 \cdot e} \quad \text{Equation 4}$$

$$e = X^{-0.22}$$ Equation 5

where Q is the source strength (in g s^{-1} NH_3), h_s the height of the source (in m), σ_y and σ_z are the standard deviation of the lateral and vertical concentration distribution respectively (in m), z_o is the roughness length (in m), T is the averaging time, and the parameters a, b, c and d are dependent on the stability classes as detailed in Pasquill (1974). The model used is a multiple plume model based on the superposition of several Gaussian plumes each described by Equation 2 to Equation 5. The concentration at each receptor is the sum of the contributions of all the sources according to Equation 1. The downwind (X) and crosswind (Y) distances are calculated for each source-receptor couple as follows:

$$X = -(x(R) - x(S)) \cdot \sin(wd) - (y(R) - y(S)) \cdot \cos(wd)$$ Equation 6

$$Y = (x(R) - x(S)) \cdot \cos(wd) - (y(R) - y(S)) \cdot \sin(wd)$$ Equation 7

Where (x(R), y(R)) and (x(S), y(S)) are the receptor and source coordinates, respectively.

These equations are identical both for the N_2O release and for NH_3 where the NH_3 source is simulated with a set of point sources. For NH_3, deposition can occur in the area between the manured circle and the measurement transect. This was evaluated during the first Oostwaardhoeve experiment and was not significant (see the Appendix).

Each manured field was described as a set of point sources. The parameter settings for the Gaussian dispersion model like receptor height, release height, z_o and stability were used as fixed values for each experimental day. Wind speed, wind direction and the location of the receptor (the mobile TDL) were obtained from measured data. There is a range of potential values for the parameter z_o and the choice of the stability class. These were set to get a good agreement between the measured and modelled lateral dispersion (width of the plume) for both N_2O and NH_3. The vertical dispersion is the most uncertain factor in the Gaussian plume model. The N_2O data was used to obtain correction factors for sets of NH_3 plumes. The factor applied was:

$$Q(NH_3) = Q(NH_{3\,model}) \cdot \frac{\Sigma\, NH_{3\,meas} / \Sigma\, NH_{3\,model}}{\Sigma\, N_2O_{meas} / \Sigma\, N_2O_{model}}$$ Equation 8

With Q the source strength for NH_3 and N_2O respectively and Σ the integral of either the measured or modelled plumes along the transect. $Q(NH_{3\ model})$ is typically fixed at 1 g NH_3 s^{-1} for each field or field strip (for the full field campaigns). When the model settings are in agreement with the actual dispersion the factor $\Sigma\ N_2O_{meas} / \Sigma\ N_2O_{model}$ will be close to unity. But since the simple Gaussian model will not include all terrain effects, for example the presence of a ditch or a line of trees between the source and receptor, this correction is required. The correction can be applied for every single plume using the individual N_2O plumes. It was found, however, that this in general increased the standard deviation of a set of subsequent emission estimates. An explanation for this is the fact that the N_2O releases are relatively close to the measurement transect (30-60 m) which makes the (point source) plumes narrow and sharp. Subsequent N_2O plumes can provide source estimates that differ by 50% or more for N_2O.

This effect is expected to be a random effect and therefore will improve when multiple measurements are combined. So in these experiments correction factors were applied per set of N_2O plumes that were linked to the same N_2O gas flask release. For a single day, two to five different releases were used.

2.2 RIVM – mobile lidar

2.2.1 Concentration measurements

The lidar and DIAL techniques

Lidar is an acronym for light detection and ranging. Its basic principle of operation is very similar to that of radar (radio detection and ranging). A short pulse of light is emitted, and any reflected light is detected and analysed. The intensity of the detected light is a measure for the amount of reflecting agents, their distance from the emitter is derived from the time difference between emission and detection.

DIAL stands for differential absorption lidar. With this technique, two or more light pulses of different wavelengths are emitted. The wavelengths are so far apart that they have different optical absorptions by the gas to be studied, yet so close that the atmosphere reflects them to the same degree. Thus, any difference in return is due to the presence of the gas to be studied. In this way, a concentration profile is obtained along the line that the light pulse travels: distance information from the return times, and concentration information from the differential absorption (Gimmestad 2005).

System design: the lidar system

The lidar system design is outlined in Figure 2-4. It consists of an emitter unit, a receiver unit, a spectrophotometer unit (not shown) and a processing and control unit (not shown). The entire system is housed in a fully self-supporting mobile laboratory.

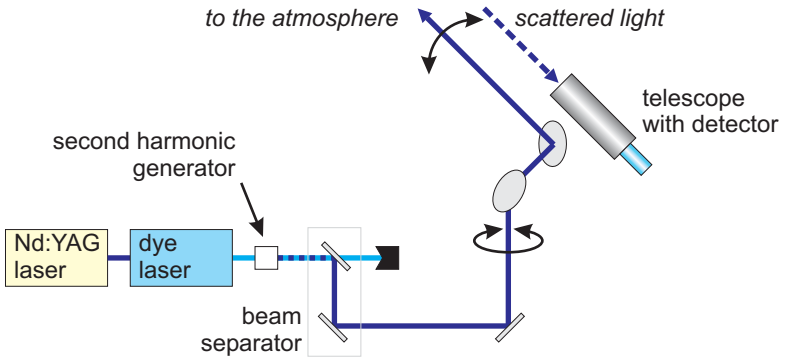

Figure 2-4. Simplified scheme of the lidar system.

The emitter unit

Light pulses are emitted by a pump laser - dye laser combination. The pump laser is a Spectra-Physics Quanta-Ray Pro 250 Nd:YAG laser. This laser runs at 30 Hz and produces pulses of 8-10 ns, with an energy per pulse of about 420 mJ at 355 nm. This light is used to pump a Sirah PrecisionScan PRSC-D-30 dye laser. This laser is equipped with a resonator, a preamplifier and a main amplifier. The

resonator is operated in single grating configuration. The grating is 1800 lines/mm and is 90 mm long. For measuring NH_3 the dye Exalite 417 is used. This configuration produces, with this dye, pulses of about 31 mJ at 417 nm. This light then undergoes frequency upconversion in a second harmonic generator to the double frequency. The resulting UV laser pulses have an energy of about 1.3 mJ, a linewidth of 1.2 pm, and a duration of about 10 ns. The divergence of the laser beam is about 0.5 mrad.

The dye laser wavelength is tuned over a wide range using a stepper motor. In addition, a piezoelectric actuator is used to rapidly detune and retune the resonator by 0.7 nm (of the fundamental wavelength). This tuning takes place between two laser pulses. In this way, the system alternates between the two wavelengths required by the DIAL technique. When measuring NH_3, the wavelengths 208.253 nm and 207.897 nm are used, for maximum and minimum light absorption, respectively. These are in the deep UV part of the electromagnetic spectrum (Figure 2-5). This is in contrast with two earlier lidar systems capable of measuring NH_3, which used light in the infrared (Force et al. 1985; Zhao et al. 2002). The maximum absorbance wavelength is known as the on wavelength, the minimum absorbance wavelength is known as off.

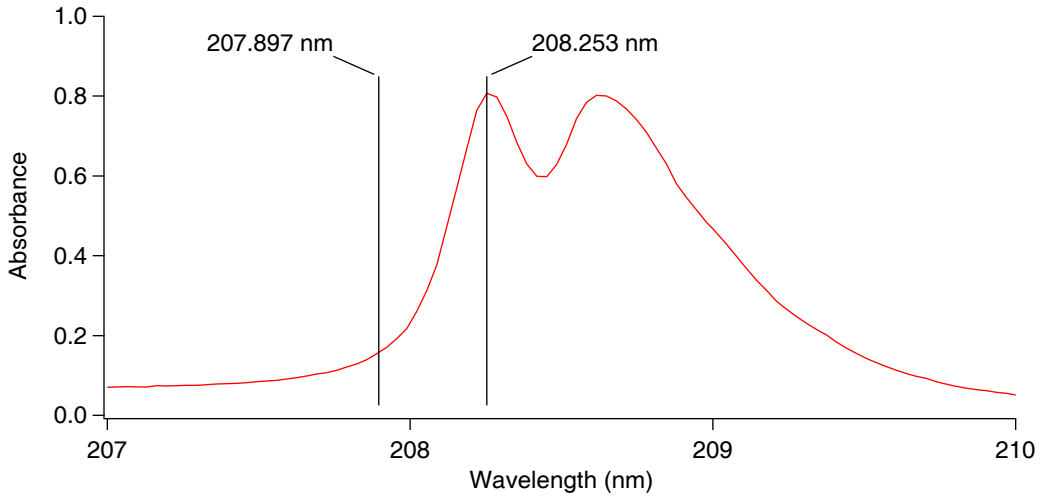

Figure 2-5. The absorption spectrum of NH_3, showing the laser wavelengths used.

The laser beam is directed to the atmosphere through a set of mirrors and prisms. The last two of these are steerable, so that the beam can be pointed at any direction around the instrument: in the vertical plane from slightly below the horizon to the zenith, in the horizontal plane almost 360º round.

The receiver unit

The receiver unit (Figure 2-6) consists of a small home-built telescope, an interference filter and a photomultiplier tube. The entire receiver is mounted on the same platform as the last mirror of the emitter unit, so that the telescope always looks in the direction that the laser beam is pointing.

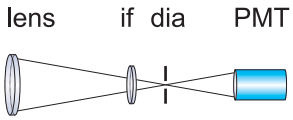

Figure 2-6. The receiver unit, if: interference filter, dia: diaphragm, PMT: photomultiplier tube.

The home-built telescope consists of a quartz lens with a diameter of 50 mm. This projects an image on the detector, which is a Hamamatsu R7400-U04 photomultiplier tube. A diaphragm limits the field of view. An interference filter blocks out any daylight by transmitting only UV light. The entire assembly is housed in a metal tube (not shown in Figure 2-6).

The telescope is placed as close as possible to the outgoing laser beam. This is to ensure that the point of full overlap is as close to the instrument as possible. The point of full overlap is the point where the outgoing laser beam is fully within the field of view of the telescope. Any signals coming in from shorter distances than that are unusable, so the point of full overlap is where the effective measuring range of the instrument starts. With this small telescope, this point lies at 35 m from the lidar.

The effective measurement range ends where the signal level drops below the noise level. For the configuration used for NH_3, this happens around 105 m. The effective measurement range is thus a mere 70 meters. This short range is mainly due to the Rayleigh scattering in the atmosphere, attenuating the light. This attenuation is proportional to the inverse of the fourth power of the wavelength. Since the wavelength used for NH_3 is very short, the attenuation is high. Other lidar applications have far longer ranges, up to 100 km or even more. Those applications use light of longer wavelengths, sometimes up to 10.6 µm.

The processing and control unit

The instrument is fully computer-controlled. All functions – instrument control, data acquisition, data processing – are handled by an integrated dedicated program, written on the LabVIEW development platform.

Data acquisition is done on a Licel 40 MHz 12 bit transient recorder. When triggered, this system acquires a record of data points spaced by 25 ns (corresponding to 3.75 m range in the atmosphere) and sums it in its memory. After a pre-defined number of triggers have been acquired, the sum is transferred to the computer and eventually stored on disc.

The mobile laboratory

The entire system is housed in a custom-built mobile laboratory, 8 m long, 2.5 m wide and 2.3 m high, mounted on a vehicle (Figure 2-7). It is fully self-contained: it has a generator, climate control and a cooling system to provide the laser with cooling water. The complete emitter and receiver units, including the steerable telescope, are mounted on a single aluminium frame (Figure 2-8). When travelling, this frame is supported by actively damping bellows, filled with pressurised air, to reduce the risk of damage due to shocks or vibrations. When measuring, the air bellows are emptied and the frame rests firmly on the laboratory floor. This floor is stabilised by underpinning the entire vehicle with hydraulically retractable supports.

Figure 2-7. The mobile lidar system, while measuring.

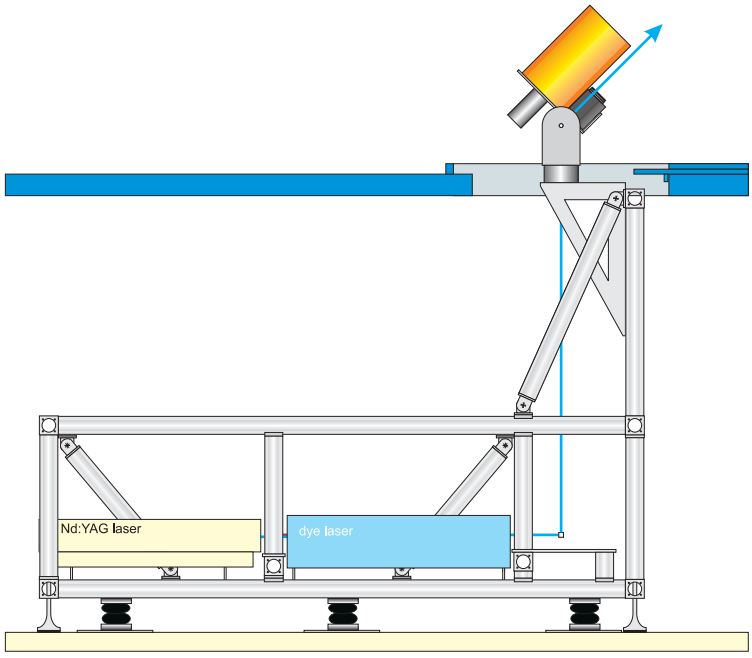

Figure 2-8. Frame with emitter and receiver units, with the telescope platform in the elevated position.

The telescope and beam steering mirrors are mounted on a retractable platform. When measuring, this is lifted out of a hatch in the laboratory roof, allowing access to the atmosphere. When travelling, it is lowered and the hatch is closed, protecting the inside from the elements.

Measurement method: single DIAL measurement
A single DIAL measurement is performed following these steps:

- The telescope and the laser beam are pointed in the desired direction.
- A number of laser shots (usually 200) are fired and the echoes are collected, as described above.

For 200 shots (i.e. 100 shots at both the on and the off wavelengths) this process takes about three seconds. A single acquisition of 200 shots, however, leads to noisy signals. To improve on this, the sequence of steps is repeated and the signals averaged. Usually, the sequence is repeated twenty times.

To calculate the concentration, the on- and off signals have their backgrounds subtracted and are divided (Equation 9):

$$\text{dial} = \ln\left(\frac{\text{background corrected on signal}}{\text{background corrected off signal}}\right) \qquad \text{Equation 9}$$

Over a suitable interval, the slope of the curve dial is determined. The concentration follows from Equation 10:

$$\text{concentration} = \frac{-\text{slope} \cdot 5 \cdot 10^{9}}{\sigma} \qquad \text{Equation 10}$$

In which σ is the molecular cross section in $cm^2\ g^{-1}$, the concentration is then given in $\mu g\ m^{-3}$. The interval over which the concentration is reported is typically 11 m. Thus, over the effective measurement range of 70 m, six concentration values are determined. For this system and this set of on- and off-wavelengths, the molecular cross section is $94.4 \cdot 10^3\ cm^2\ g^{-1}$.

2.2.2 Meteorological data

The wind profile is obtained by simultaneously measuring the wind speed at three different altitudes, usually at 0.85 m, 3.3 m and 5.5 m. On a telescoping mast (Figure 2-9) three MMW-005 solid-state anemometers from Mierij Meteo are mounted. They measure both wind speed and wind direction. The wind directions are averaged. Through the wind speeds, a logarithmic profile is fitted. This profile is used in the calculations described earlier.

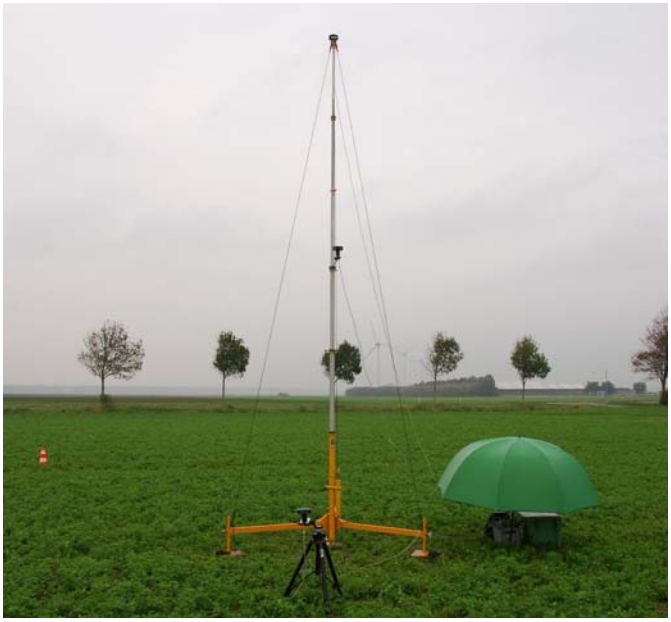

Figure 2-9. Wind measurement mast at the Oostwaardhoeve. The umbrella is to protect the data acquisition computer.

This three-point wind measurement system is not present on all days. When it is not, a single wind meter is used. In those cases, to calculate a vertical profile, a logarithmic wind profile (Stull 1988) is assumed.

2.2.3 Emission calculation

To determine the emission of a manured field from a set of concentration measurements the following procedure is adopted. The lidar measures a set of directions, all in the same horizontal direction but with increasing elevations. This way, an image of the NH_3 concentration distribution in a vertical plane is obtained. This plane is positioned downwind from the manured field, so that the wind carries any emitted NH_3 through it. See Figure 2-10 for a scheme showing the set-up.

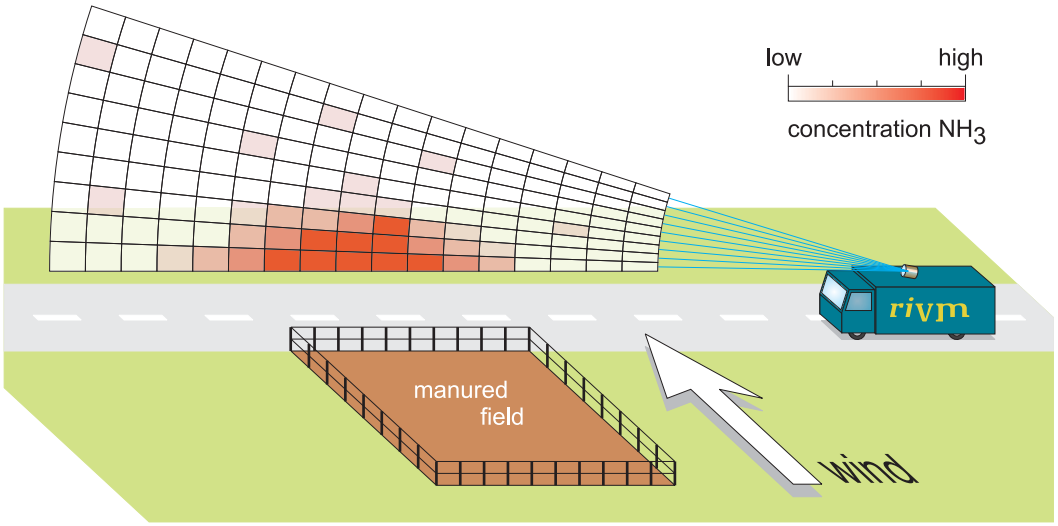

Figure 2-10. Scheme showing how the NH_3 emission of a manured field is measured.

From the two-dimensional concentration distribution the gas burden curve is calculated. This is achieved by summing all concentration values on the same altitude. It is expressed in mass units per surface units. This gas burden curve is multiplied with the wind speed profile (see section 2.2.2 above). The product is summed to arrive at the total flux of NH_3 passing through the vertical plane, per unit of time. By convention, in the Results section below, all fluxes are reported as g NH_3-N s^{-1}.

In order to be able to compare emissions as determined by the lidar with emissions determined through other methods, the flux is divided by the emitting surface. The emission is then reported in g NH_3-N s^{-1} ha^{-1} (1 ha = 10^4 m^2). This step requires knowledge of the emitting surface. If the field is small, as depicted in Figure 2-10, all NH_3 emitted by the field passes through the measurement plane. In this case the emitting surface equals the total surface of the manured field. If the field is large, only the NH_3 from a sub-section of the field is observed by the instrument. In the sections pertaining to the individual experiments the methods used to determine the emitting surface are elaborated.

To further facilitate comparison of the results, the cumulative emissions are expressed in percent of applied TAN, i.e. the percentage of the Total Ammoniacal Nitrogen applied. The latter quantity is known through measuring or estimating the manure application rate and chemical analysis of manure samples, taken during manure application.

2.3 WUR – micrometeorological mass balance method

2.3.1 Concentration measurements

The volatilization of NH_3 following manure application is determined per plot using the micrometeorological mass balance method (Denmead 1983; Ryden and Mcneill 1984) as applied by Huijsmans et al. (2001). The manure is applied on a circular plot with a radius varying from 20 to 24 m. The circular plot is created by applying the manure over a pre-marked area in parallel passes that vary in length (Figure 2-11). The circular plot is created to achieve an equal fetch length to the centre of the plot, when wind direction changes.

Shortly after the manure is applied to the first half of the plot – which usually is within five minutes after the start of the manure application – a mast supporting five NH_3 traps between 0.25 and 3.30 m above ground level is placed in the centre of the experimental plot (Figure 2-11). At the windward boundary of the plot another mast is placed with three NH_3 traps at heights between 0.40 and 2.30 m above ground level. At the boundary, fewer traps are used because the background concentration is low and independent of height. Each trap contains 20 ml of 0.02 M HNO_3 held in 100 ml collection tubes. Air is drawn through the acid solution via a stainless steel inlet tube with a perforated Teflon cap. The volume of air is measured with flow meters. Flow rate is 2 to 4 dm^3 min^{-1}. Ion-chromatography and colorimetry are used to measure the NH_4^+ concentration in the solutions.

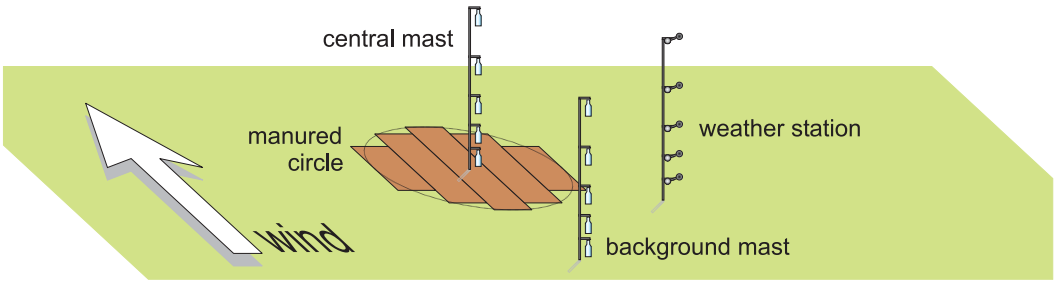

Figure 2-11. Layout of circular plot (diameter about 50 m) for the measurement of NH_3 volatilization using the micrometeorological mass balance method, with masts supporting NH_3 traps at various heights in the centre of the plot and at the windward boundary of the plot.

In general the measurements continue for at least 96 hours after manure application. During the first twelve hours – when the rate of NH_3 volatilization is highest – traps are replaced four to five times. Further replacement takes place every morning for the following four days. The amount of NH_3 volatilized during each interval is estimated from the amount of NH_3 trapped, and from the airflow data.

2.3.2 Meteorological data

Wind speed is measured with five cup anemometers placed at different heights to calculate a good wind profile at the experiment location. The meteo mast is placed close to the manured plot in the open field (Figure 2-12).

Figure 2-12. Meteo mast to measure wind speed at five heights. In the background the central mast in the manured plot.

2.3.3 Emission calculation

The micrometeorological mass balance method is based on the law of conservation of mass. The flux from an emitting surface is determined from differences in the mass of gas (NH_3) carried by the wind across the upwind and downwind boundaries of an experimental area (field plot). In the absence of NH_3 upwards of the field plot, the ammonia flux F from a field can be calculated according to:

$$F = \frac{1}{x}\int_{z_0}^{z_p}(\bar{u}(z).\bar{c}(z) + u'(z).c'(z))\,dz \qquad \text{Equation 11}$$

where F is the vertical NH_3 flux (in g m^{-2} s^{-1}); x is the fetch length (in m), that is the distance the wind is travelling across the field plot from the windward boundary of the field to the measuring point (the central mast); z_p is the height (in m) at which the ammonia concentration equals the background concentration; z_0 is the roughness length, that is the height (in m) at which the wind speed u equals 0; u(z).c(z) is the average horizontal flux in time caused by horizontal convection at height z of the central mast (in g m^{-2} s^{-1}); and u'(z).c'(z) is the turbulent flux caused by horizontal diffusion perpendicular to the wind direction (in g m^{-2} s^{-1}).

In general it is assumed that the turbulent flux can be neglected compared to the convection term, resulting in:

$$F = \frac{1}{x} \left(\int_{z_0}^{z_p} \bar{u}(z) \cdot \bar{c}_2(z)\, dz \right)$$ Equation 12

In the presence of NH_3 sources windward of the field plot, the NH_3 concentration profiles both upward of the experimental area (background) and in the central mast need to be determined. These NH_3 concentration profiles are then combined with a wind speed profile to obtain an integrated horizontal NH_3 flux at both positions. The net NH_3 flux from the field plot can then be calculated as the difference between the fluxes through both vertical planes:

$$F = \frac{1}{x} \left(\int_{z_0}^{z_p} \bar{u}(z) \cdot \bar{c}_2(z)\, dz - \int_{z_0}^{z_p} \bar{u}(z) \cdot \bar{c}_1(z)\, dz \right)$$ Equation 13

where F is the vertical NH_3 flux (in g m^{-2} s^{-1}); u(z) is the wind speed (in m s^{-1}) at height z; c1(z) is the average background NH_3 concentration (in g m^{-3}, windward of the field plot) at height z; and c2(z) is the average NH_3 concentration (in g m^{-3}) at height z of the central mast.

For both wind speed and NH_3 concentration a logarithmic profile is assumed:

$$u = D + E \ln(z)$$ Equation 14

$$c_2 = A + B \ln(z)$$ Equation 15

The model approach is based on the statistical analysis of the NH_3 volatilization rate during the various measuring intervals after application and incorporation of the manure. NH_3 volatilization was measured with the mass balance method as described in section 2.3.1. The analysis was carried out on a large number of experiments (58 plots and 503 measuring intervals) in which NH_3 volatilization was measured during 96 hours after manure application. The analysis and model development was carried out to reveal the effects of application method, characteristics of the manure, characteristics of the weather conditions and characteristics of the field. The mean volatilization rate in a measuring interval was assumed to be the actual value at time t, being the time at the middle of the interval. The basic equation used to describe the logarithm of the volatilization rate of application method k $z_k(t)$ at time t after application is:

$$\ln z_k(t) = \alpha_0 + F_k + \alpha_t \ln(t) + \Sigma\, \alpha_m x_{mt}$$ Equation 16

where α_0 is a constant, F_k the model factor for application method, t the time elapsed since the manure was applied, α_t the coefficient for the term ln(t), α_m the coefficient for the term x_{mt}, x_{mt} the model term for explanatory variable m at time t.

The model approach allows for utilizing the measured characteristics of the weather conditions per measuring interval as explanatory variables in a statistical model for the volatilization rate (expressed as kg NH_3-N ha^{-1} h^{-1}). This approach also allows for inclusion into the model of the change in characteristics of soil and manure in the period after application, that may be related to the observed

decline in volatilization with time. As the change in TAN content of the manure (depletion of the source due to volatilization) could be calculated from the data, the adjusted total ammoniacal nitrogen content (ATAN) is used in the analysis. Other data on changes in characteristics of the manure or the soil, such as TAN lost from the available pool by infiltration, adsorption or biochemical changes, were not available.

The effect of application technique or incorporation technique on volatilization turned out to be strong, and was therefore included into the model. The logarithm of time after manure application was included in the model because the decline of the volatilization rate with time could not be fully explained from the change in NH_3 content (ATAN). Other factors considered for inclusion into the equation were weather conditions (wind speed, air temperature, relative humidity, radiation), soil type (sand, sandy loam, clay), soil moisture content, manure characteristics (ATAN content, dry matter content), application rate, and stubble height.

Statistical analysis of the effect of the various factors that could explain the observed volatilization rates, using Equation 16, revealed that the volatilization rate was significantly affected by the method of application and incorporation, the ATAN content of the manure, the manure application rate, the wind speed and the ambient temperature. An interaction effect was found for wind speed and application method. The selected equation, in which only the significant factors were included, was:

$$E(\ln z_k(t)) = \alpha_0 + F_k + \alpha_t \ln(t) + \alpha_1\ ATAN + \alpha_2\ rate + \alpha_3\ wind + \alpha_4\ temp + F_{kw}\, wind \qquad \text{Equation 17}$$

Descriptions, estimates and standard errors of the model parameters are statistically estimated. The model is based on experiments with the mass balance method. In these experiments ammonia volatilization was measured for a period of 96 hours after manure application. Model parameters are based on this period after manure application.

The factors causing variation between the experiments and variation in volatilization rate within the period after application were analysed. Important factors were identified and their effect on the NH_3 volatilization rate was estimated. Uncertainty remains about the predictions and subsequent calculations made with Equation 17. This uncertainty is reflected by the relatively large confidence intervals of predictions of the total volatilization for a certain application method at a random location and a random point in time.

2.4 Emission measurements experimental set-up

On a measurement day, the following activities are taking place.

Preparation
ECN, when present, set up the N_2O release system, their anemometer and the Amanda wet annular denuder (when present). They then start driving the mobile TDL system as described above, up and down, downwind from the area to be manured.

RIVM set up their anemometer mast and position the mobile lidar. They then start measuring, to determine the background concentration.

WUR set up a premarked circular plot and take care of manure application.

Manure application
While all systems are measuring, the manure is applied. If the micrometeorological mass balance method is used, its central mast is placed in the centre of the plot and ammonia measurements are started at both masts, halfway through the manure application. **WUR** takes samples of the manure as it is being applied, often of each batch, if there is more than one.

Measurement
After all manure has been applied, the measurements continue for some time. This varies from several hours to several days. The extend of the manured area is mapped.

Other activities
On some days, additional activities are taking place. These are listed in the Results and Discussion section.

2.5 Manure analysis

During the experiments manure samples were taken and the manure application was measured by weighing the manure tank before and after manure application (for the experiments involving circular plots) or by counting the number of tank loads that were applied. The total ammoniacal nitrogen applied was calculated from the manure load applied, the manure analysis and the surface area on which the manure was applied.

3 Results and discussion

3.1 Measurement locations

During the campaign described in this report, measurement activities were deployed on three locations. Figure 3-1 shows maps for each of these locations, and their positions in the Netherlands. Table 3-1 lists all measurement days.

Table 3-1. Measurement days.

date	**location**	**NH_3 source**	**measurements**	**land type**
09-08-2006	Amsterdam	artificial source	TDL, lidar	asphalt
18-10-2006 to 19-10-2006	Oostwaardhoeve	manured circle	TDL, lidar, manure samples	arable
14-03-2007 to 17-03-2007	Oostwaardhoeve	manured circle	TDL, lidar, mass balance, manure samples	arable
27-03-2007	Oostwaardhoeve	manured field	TDL, lidar, manure samples	arable
03-08-2007	Woerden	manured field	TDL, Amanda, lidar, manure samples	grassland
10-08-2007	Woerden	manured field	lidar, manure samples	grassland
13-08-2007	Woerden	manured field	lidar, manure samples	grassland

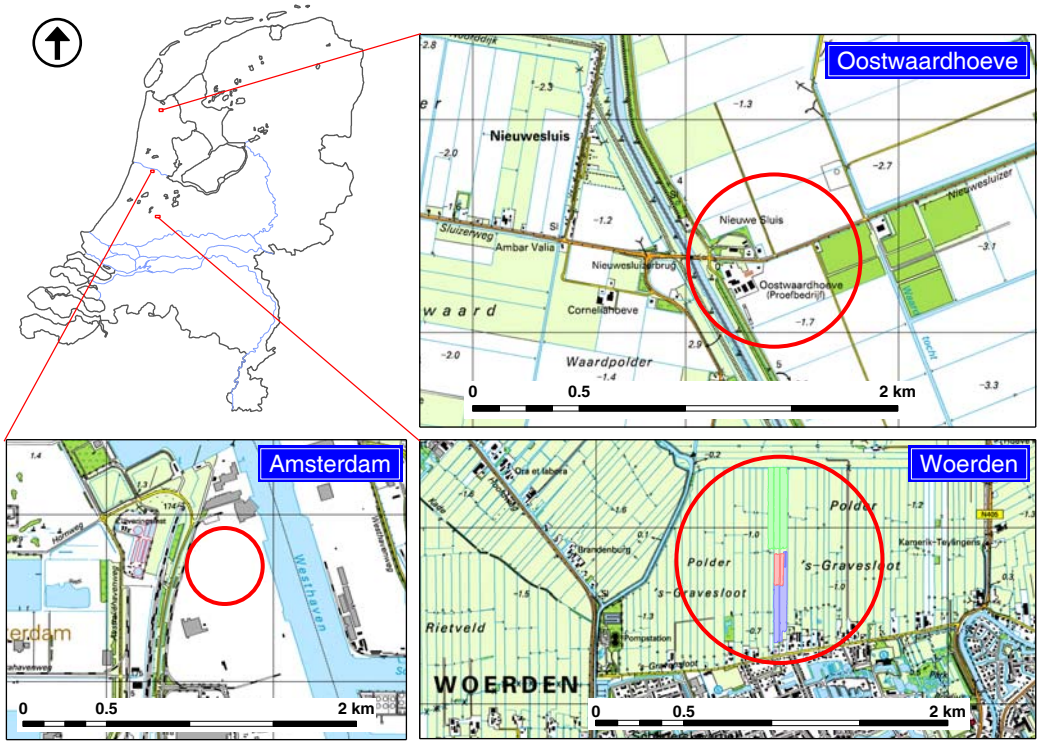

Figure 3-1. Measurement locations.

In **Amsterdam**, in the harbour area to the West of the city, a suitable site was found to measure the NH_3 emission from an artificial source. It is a large asphalted site, used for storing imported vehicles. There were no significant other NH_3 sources in the vicinity. When the emission measurements took place, on 9 August 2006, it was empty.

The **Oostwaardhoeve** is an experimental arable farm, situated in the West of the Wieringermeer polder. All measurement activities described in this report took place on the same field, which had been used during the previous season to grow alfalfa. On the first two measurement occasions, a small circular plot on this field was manured. On the last measurement day on the Oostwaardhoeve, the entire field was manured.

Woerden lies in the very heart of the Netherlands. The experiments there took place on a commercial dairy farm. Its fields are permanent grassland. The land is manured, then grazed by cows, and/or the grass is mown to be stored for winter fodder. These cycles are repeated several times during a growing season. Measurements were taken on three days, when the strips of land indicated in Figure 3-1 and in Figure 3-26 were manured.

3.2 Artificial ammonia source – Amsterdam, 9 August 2006

3.2.1 Experimental set-up

On 9 August 2006, test measurements were performed on an artificial NH_3 source. These measurements were carried out to evaluate the capabilities of the TDL and the lidar systems to measure

NH_3 emissions. On the large asphalted area described above, TNO set up a NH_3 release system (Figure 3-2, Figure 3-3 and Figure 3-4). This system consisted of three concentric circles of tubing, with spouts at regular intervals. A mixture of NH_3 and nitrogen from a gas cylinder was led through these tubes and released into the atmosphere. The diameter of the outer circle was 50 m. The NH_3 emission from this system was 0.50 ± 0.04 g NH_3 s^{-1}. This emission was controlled with a mass flow controller, and checked by weighing the gas cylinder at regular intervals.

Participants on this day were ECN, with the TDL and with a wind meter; RIVM, with the mobile lidar and with the wind meter mast (although in the morning, only a single wind meter was used); and TNO, with the NH_3 release system. Because the wind changed direction during the day, some of the apparatus was moved half-way through the day. The situation is shown in Figure 3-2. The TDL tracks shown in this Figure were chosen so that they transected the emitted NH_3 plume. The mobile lidar was sited so that the wind carried the plume through its measurement plane.

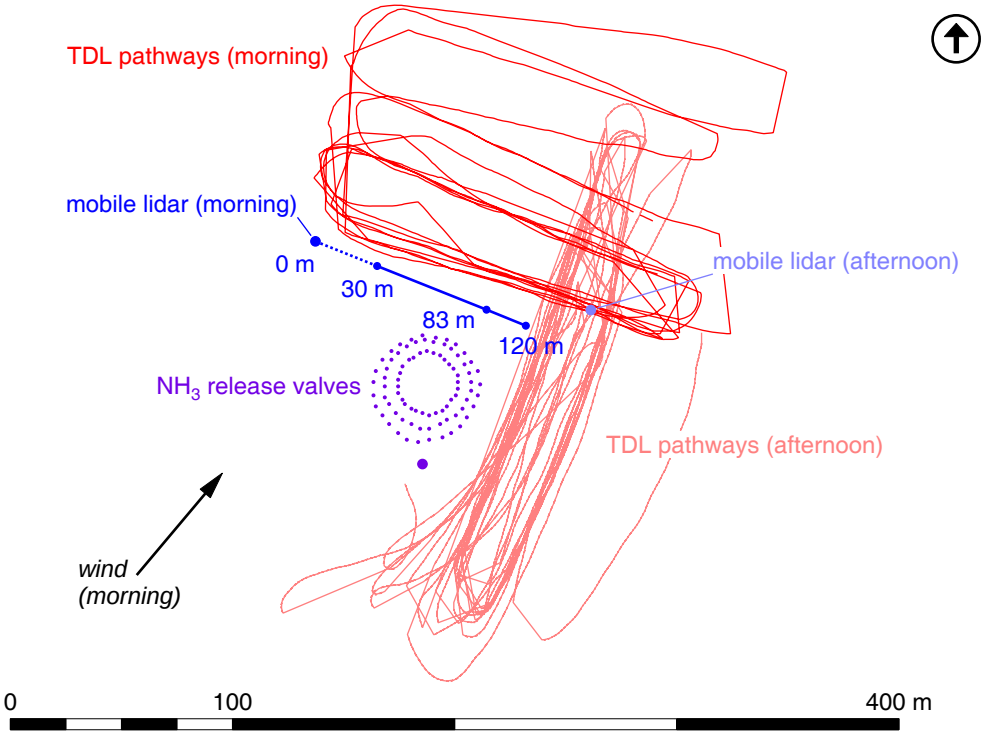

Figure 3-2. Amsterdam, the situation on 9 August 2006.

Figure 3-3. The mobile lidar (left), the NH_3 release system (middle and foreground) and the mobile TDL (right).

Figure 3-4. The NH_3 source.

3.2.2 Measurement results

Meteorological conditions

Figure 3-5 shows the wind meter results for both wind meters present. The data for the RIVM wind meters after 12:00 is averaged from the three wind meters present.

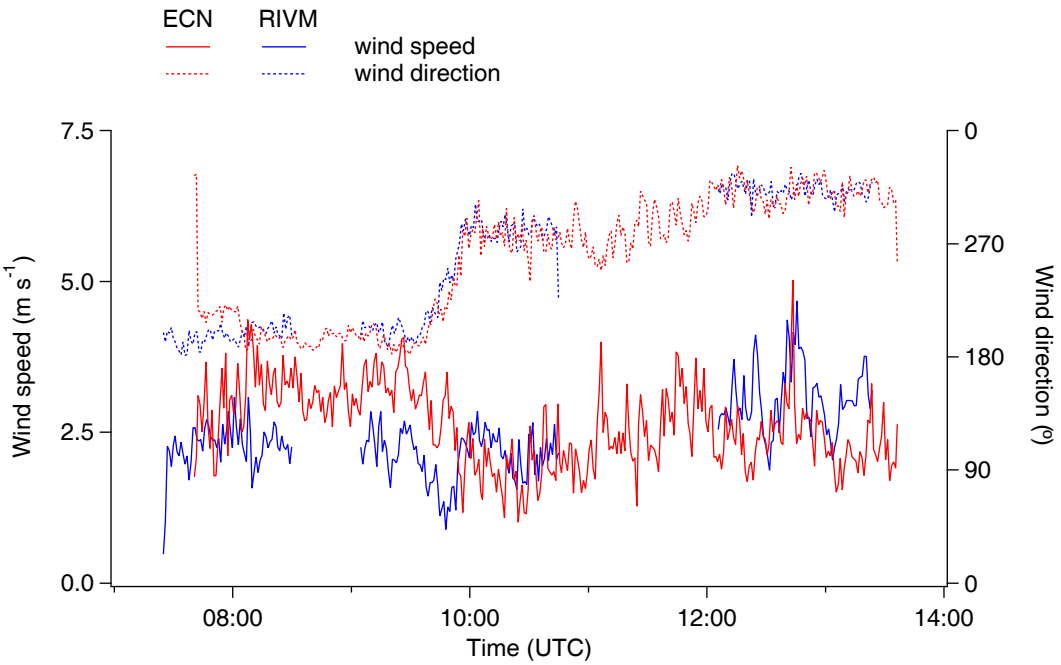

Figure 3-5. Amsterdam, wind speed and wind direction on 9 August 2006. Data interval reduced to 1 minute. Wind meter altitude: 1.8 m (ECN), 1.5 m (RIVM, morning) and 2 m (RIVM, afternoon).

When analysing the wind meter data, it turned out that, in the morning, the RIVM wind meter was not well sited; it had been placed in the lee of a fence. The ECN wind meter had been positioned better. In the afternoon the situation was reversed. The variability in the wind direction increased in the afternoon when the wind had moved from south to west.

Concentration and emission measurements

The TDL NH_3 measurements were calibrated versus the on-board Airrmonia in this experiment. Settings for the plume model for z_0 and stability were chosen using the two different sets of transects. The settings for the model were set to get a good agreement of the decay of the plume versus distance. In this experiment the transects though the plume could be obtained on several distance from the source which is in general not possible in the agricultural area.

Figure 3-6 shows the results for one of the measurements performed by the mobile lidar. This measurement was taken between 08:57 and 09:31 UTC. The left graph shows the wind profile. As discussed above, the wind meter from ECN was better sited than the one from RIVM, therefore, the profile reported in the Figure is based on the ECN wind meter. Since only one wind meter was present, this profile was calculated from the measured wind speed assuming a logarithmic wind profile. The surface roughness length used in the calculation was 0.001 m.

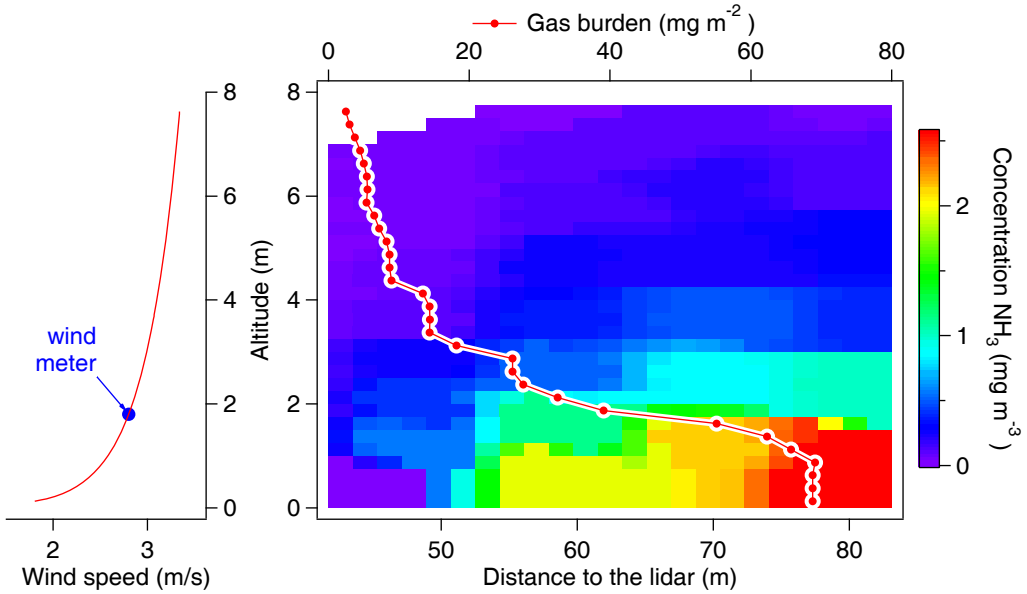

Figure 3-6. Amsterdam, 9 August 2006, wind profile (left) and plume cross section with gas burden curve (right). Measurement taken between 08:57 and 09:31 UTC.

The right-hand graph shows the concentration cross section through the emitted plume. Overlaid on this is shown the gas burden curve.

Emission results

TNO released NH_3 with an average emission of 0.50 ± 0.04 g NH_3 s^{-1} (95% confidence interval at n=39).

The average source strength obtained with the TDL, based on the results of 27 plumes was 0.47 ± 0.11 g NH_3 s^{-1} (95% confidence interval at n = 27).

Using the lidar data with the curve shown above, and from the wind speed profile, the emission value of 0.49 g s^{-1} was calculated. However, it is likely that this number does not represent all of the emission. The plume as released by the artificial source should be 50 m wide. As can be seen in Figure 3-6, only some 28 m are actually seen. The plume would have been expected to continue to the right of the vertical slice, outside the measurement range of the lidar. Because the section of the plume that is mapped is only half the expected width, it seems reasonable to assume that the section that is measured is only half of the plume released. This would mean an emission value of 0.98 g NH_3 s^{-1}.

Figure 3-7 shows the emission rates as measured by the TDL and by the lidar. It also shows the source strength as derived from the release parameters by TNO, both volumetric and gravimetric. Note that this graph shows emissions in g NH_3 s^{-1}. The TDL and lidar emissions shown are averaged, the interval over which the averaging has taken place is indicated by the lengths of the horizontal lines.

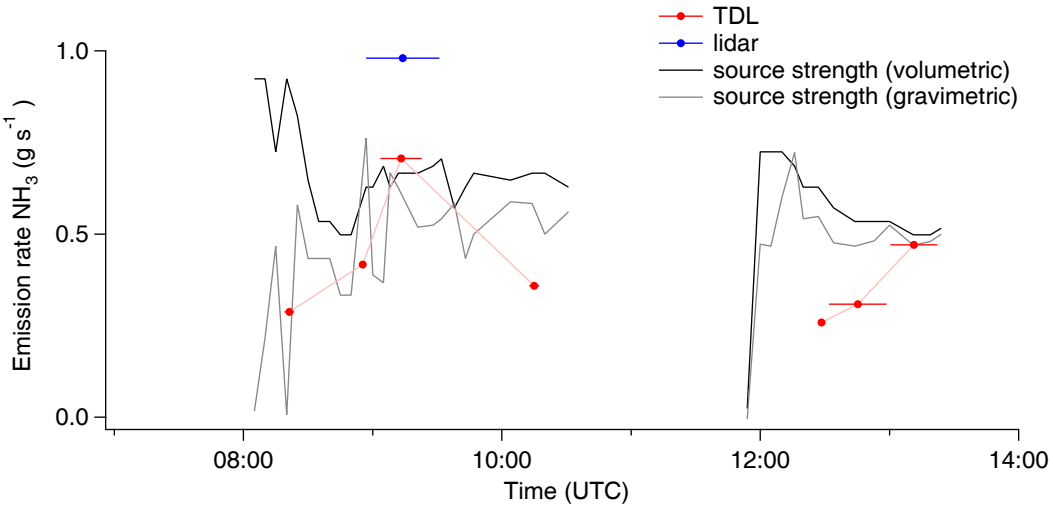

Figure 3-7. Emission rates as measured on the artificial ammonia source, Amsterdam, 9 August 2006. The TDL 30 minute grouped emission data has an average of 0.47 g s^{-1} taking into account the number of plumes in each 30 minute bin.

Table 3-2. Emission estimates (in g s^{-1}) measured with the TDL.

time	average	standard deviation	number of measurements
8:30	0.29	0.22	2
9:00	0.42	0.15	3
9:30	0.71	0.34	9
10:30	0.36	0.14	2
12:30	0.26		1
13:00	0.31	0.17	7
13:30	0.47	0.41	3
total	0.47	0.30	27

The average of all individual emission data points is 0.47 g s^{-1}. It can be argued that this is a biased average due to the high values obtained around 9:30. When all data is binned in 30 minute intervals and the average over these intervals is used (as shown in Table 3-2) a level of 0.40 g s^{-1} is found. This is 20% below the level reported by TNO.

3.2.3 Discussion

The aim of these experiments was to test the ability of the lidar and TDL instruments to measure NH_3 emissions. For the TDL, the emission results are in line with the expected values however, the poor siting of the wind meters added uncertainty to the emission values. This uncertainty was not quantified.

With the lidar, only a single emission value was determined. It is considerably higher than the average source strengths determined by TNO, and higher than the emission measured by the TDL as well. The two most conspicuous factors that make interpretation of the lidar results difficult are the poor wind meter siting and the large size of the ammonia plume. The problems concerning the placement of the wind meters were discussed in section 3.2.2 on page 37 and add uncertainty to the emission number.

However, because the same wind speed and direction were used for the interpretation of both the lidar and the TDL results, any deviation would have been expected to be in the same direction. This seems not so likely, as the TDL emission value measured at the same time as the lidar value coincides well with the TNO values.

Why the large size of the ammonia plume is problematic for the lidar was discussed in section 3.2.2 on page 38. This problem is exclusive to the lidar, because the TDL was able to capture the entire plume. Therefore, it is recommended that this artificial release experiment is repeated, but with an emission circle of 25 m radius. Combined with better sited wind meters, this is expected to lead to better, unambiguously interpretable results. The successful measurements on manured circles of 25 and 35 m diameter at the Oostwaardhoeve (see sections 3.3 and 3.4) suggest that such an experiment is feasible.

3.3 Manured field section 1 – Oostwaardhoeve, 18-19 October 2006

3.3.1 Experimental set-up

This experiment was carried out at the Oostwaardhoeve on 18 and 19 October 2006 (Figure 3-8). The TDL and mobile lidar measurement techniques were used to measure the NH_3 emission from a manured circular plot. A relatively small – 24 m diameter – experimental plot was used, so that the lidar would be able to measure the complete emitted plume.

Figure 3-8. Manure application on the Oostwaardhoeve, 18 October 2008. In the background the lidar.

Manure was applied on the circular plot with a diameter of about 24 m on bare arable land with an alfalfa stubble. The circular plot was created by applying the manure over a pre-marked area in parallel passes that varied in length (Figure 2-11). The amount of manure applied to the plot was measured by weighing the manure tank before and after application. After manure application the manured area was measured by measuring the length of the parallel passes and the width of the passes. The plot area was 629 m^2. The manure was surface applied (Figure 3-8). Surface spreading was carried out by a tanker fitted with a shallow injector for arable land. The injector had a working width of 4 m and was kept about 30 cm above the soil while applying the manure. In combination with the high application rates in this experiment a situation of surface spreading was achieved. The application rate was 49.6 m^3 ha^{-1}.

The high application rate was applied to achieve high volatilization rates in this experiment. Pig manure was applied, which was imported from pig farms by a contractor. Three manure samples were taken by WUR while the tanker was applying the manure on the field. The manure was afterwards analysed for pH, dry matter and TAN content. On average, this pig manure contained 3.81 g TAN and 76.2 g dry matter per kg, and had a pH of 7.6.

All measurements started before the manure was applied. This application took place from 12:54 to 13:05 UTC. At the end of the day, shortly before dark, the measurements were stopped and all apparatus was removed. The next day, all instruments were returned to their original positions and measuring was resumed. This continued for several hours.

RIVM contributed their three wind meters on a mast, and the mobile lidar. The latter was positioned to the northeast of the manured plot; it measured almost due west. See Figure 3-9 for an overview of the situation.

In addition to the RIVM mast with three solid state wind sensors, ECN operated their single sensor as well. However, comparison of the data of that sensor with the data of the three RIVM sensors showed that the wind speeds it measured were too high. Therefore, its data is not reported here, and it was not used in the analysis of the TDL data. Instead, ECN used the RIVM data. After the experiment, the sensor was replaced.

ECN was present with their single wind meter, their N_2O release system, and the mobile TDL. The N_2O release system was placed close to the manured plot. It released N_2O from a single gas flask using a critical capillary at 1 bar prepressure. Release rates were derived from the flask weights before and after the experiment, and were about 0.5 g N_2O s^{-1}. ECN chose the public road running to the north of the field to drive the mobile TDL system up and down. This resulted in southwest-northeast transects about 60 m north of the manured circle (Figure 3-9). The TDL concentration data were calibrated using air from a gasbag with 200 µg m^{-3} NH_3 that was measured both on the Airrmonia and the TDL. A calibration factor of 1.14 was obtained. A tailing correction was applied which should correct for the effect of the long inlet line. Since measurements were carried out on a busy road the vehicle could not drive backward (this was possible during the second experiment on 14 to 17 March 2007, discussed in section 3.4 below). Therefore, depending on the driving direction, the inlet was at the front of the car but still either upwind or downwind of the vehicle. Since the plumes were only 20-30 m in width, the size of the van (6 m long) caused a significant disturbance. This was reflected in the estimated emission with a 30% difference depending on the driving direction. For the third experiment at the Oostwaardhoeve (27 March 2007, see below), when the whole field was manured and plumes were more than 50 m wide, no difference was observed when the inlet was at the upwind or downwind side of the car.

Plume modelling

The model used z_o=0.1 and a stability class in between Pasquill C and D at an average time of T = 0.03 hours. At these settings the crosswind dispersion (width of the plumes) agreed best with the observed values both for the N_2O and NH_3 plumes. Final correction of the NH_3 emission estimate was done with the ratio between the N_2O emission factors estimated by the model and the known average N_2O emission factors per flask release. These corrections were between 10 and 30%.

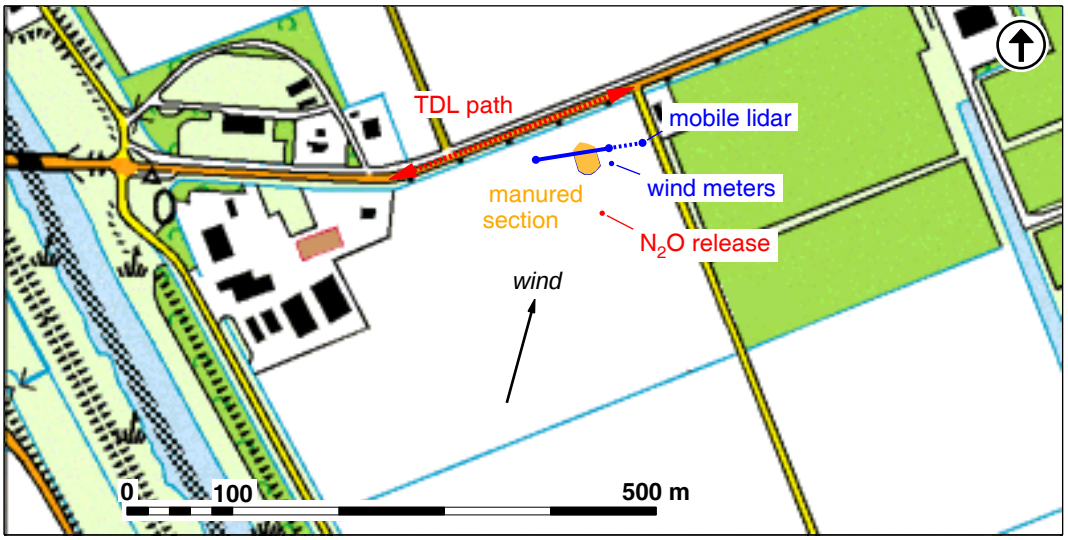

Figure 3-9. Oostwaardhoeve, the situation on 18 and 19 October 2006.

3.3.2 Measurement results

Meteorological conditions

The results of the wind measurements are shown in Figure 3-10. Wind speed and wind direction were measured at three altitudes. For each measurement, a logarithmic fit through the three simultaneously measured wind speeds was performed. From this fit, the wind speed at 2 m altitude was calculated and plotted in the graph. The wind direction was the average of the three directions measured at the three altitudes. Both speed and direction were measured about three times per second; the values shown in Figure 3-10 were averaged to one value every minute.

The grey shading in the background of the graph denotes the day (white) and night (grey) periods. The smooth transition between the two is the period of civil twilight, when the sun is less than 6° below the horizon. Also indicated in the graph is the period when the manure was applied onto the field.

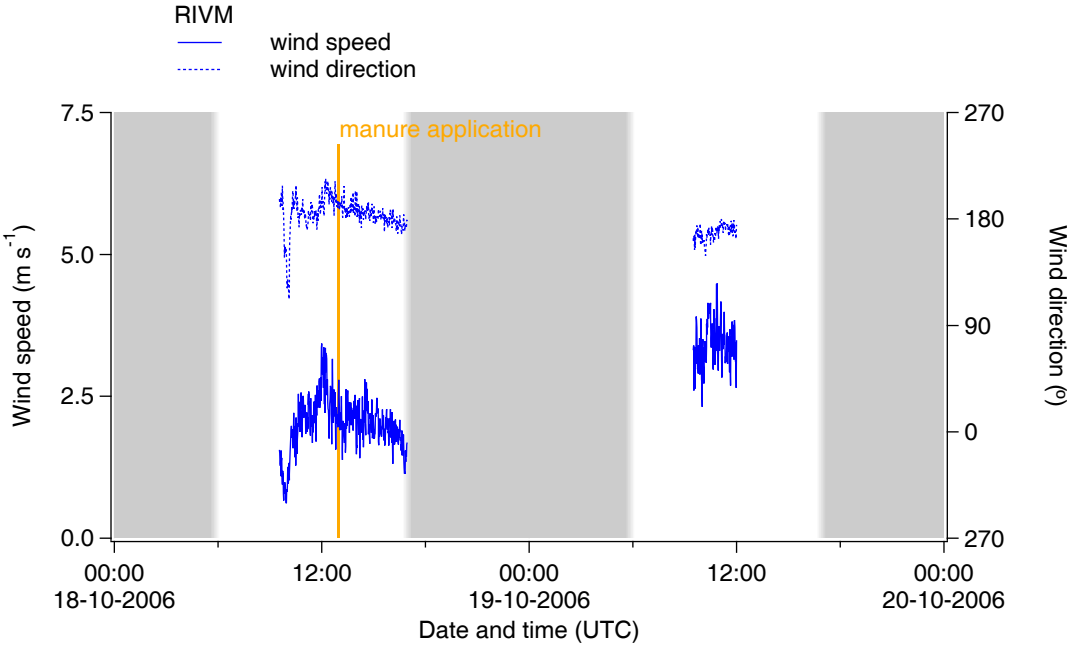

Figure 3-10. Oostwaardhoeve, wind speed and wind direction on 18 and 19 October 2006.

Concentration and emission measurements

Figure 3-11 and Figure 3-12 show the emission rates for these two days, as measured with the TDL and lidar instruments. The values are plotted on the left axis, and are expressed in g NH_3-N s^{-1} ha^{-1}; 1 g NH_3-N reads as “one gram of nitrogen originating from ammonia”. Day and night periods, as well as the period of manure application, are indicated, as they are on the wind graph (Figure 3-10).

Both emission rates are integrated to yield the cumulative emission. This is expressed as a percentage of the total applied ammoniacal nitrogen (TAN). The latter figure is derived from the chemical analysis of the applied manure, for this experiment, it amounted to 189 kg NH_3-N ha^{-1}. The cumulative emission is plotted on the right axis.

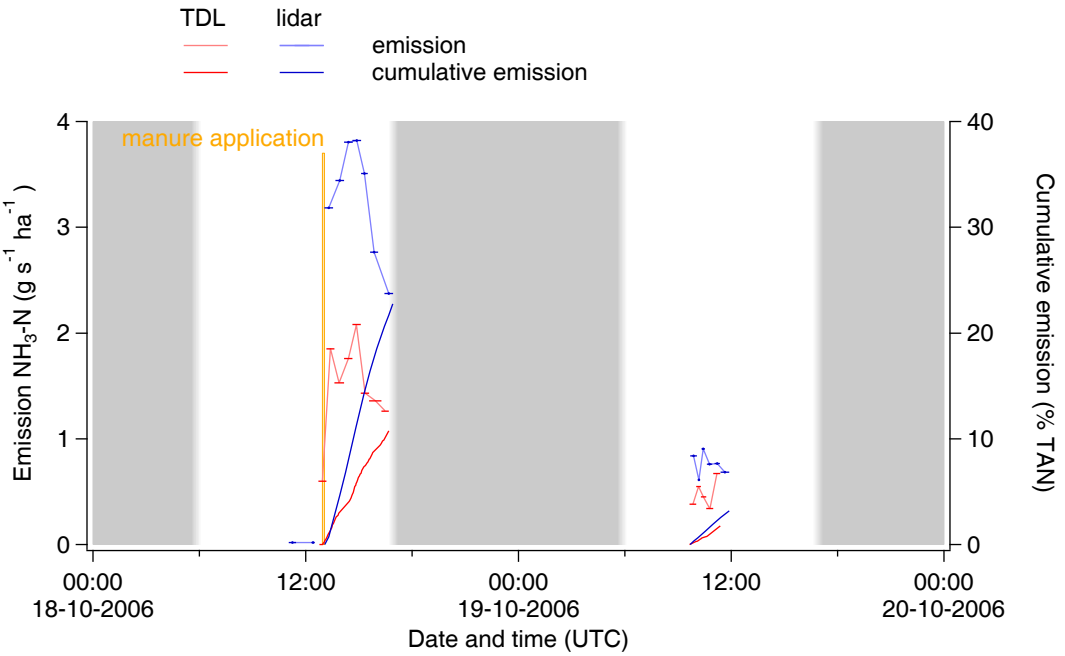

Figure 3-11. Oostwaardhoeve, graph showing the nitrogen emission rate (left axis) and the cumulative nitrogen emission (right axis) on 18 and 19 October 2006. Note: 100% TAN corresponds to 189 kg NH_3-N $\cdot ha^{-1}$.

The emission measurements performed the day after the manure application were also integrated. Because the emission in the intervening period was not known, the cumulative emissions for this day were reset to zero before integrating.

In Figure 3-12 the same data is shown as in Figure 3-11, but zoomed in on the first day of the measurements.

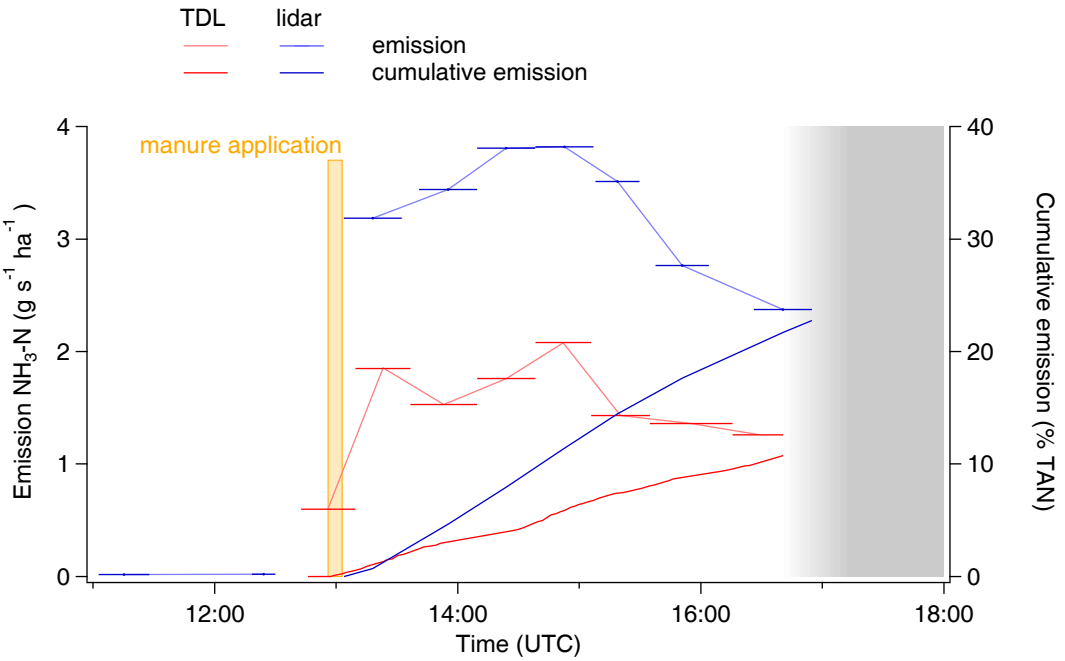

Figure 3-12. Oostwaardhoeve, graph showing the nitrogen emission rate (left axis) and the cumulative nitrogen emission (right axis), zooming in on 18 October 2006.

3.3.3 Discussion

The emission rate as measured with the lidar had its maximum some two hours after manure spreading had ended. After those two hours, the emission rate started to decline. On the second day, the lidar measured a considerable emission, even though measurements then lasted a mere two hours. The cumulative emission measured then amounted to 14% of the cumulative emission measured on the first day.

The emission obtained from the TDL measurements were below those observed by the lidar. The TDL data do agree with pattern shown by the lidar, of an increase in the emission for some time after the end of manure spreading, followed by a steady decrease. This is different from the behaviour that might be expected, with the highest emissions occurring immediately after spreading, and a subsequent decrease.

Since the TDL measurements were done at about 50 m downwind of the manured plot, deposition in the area between the manured circle and the TDL transect might have occurred. This effect is discussed in the Appendix. Deposition will only have lowered the measured concentration levels with about 3% so this cannot explain the large difference between the TDL and lidar measurements. The TDL emission estimates for this experiment are thus clearly too low. This was probably caused by the long inlet tube that has damped the NH_3 peak concentrations, in spite of the tailing correction which was applied to compensate for this effect. As discussed above (see section 2.1.1 on page 16), this long inlet tube was used to enable sampling in front of the van. Its other purpose was to be able to evaluate the effect of different inlet heights.

On the second day the lidar and TDL measured similar emissions, which were some 16% of the level observed with the lidar on the first day. At this day TDL measurements started with the long inlet tube used on the first day again, but no NH_3 was observed at all. After some tests the inlet tube length was reduced to 1 m. From that moment on, successful measurements could be performed.

When the measured cumulative emission curves are compared to the modelled cumulative emission, two things are observed. First the shapes of the curves. Both the TDL and the lidar measurements show a slow start.

To summarise: the TDL shows emissions much lower than the lidar and the model, but this is probably due to the long inlet tube. Both TDL and lidar measure a significant emission on the second day.

3.4 Manured field section 2 – Oostwaardhoeve, 14-17 March 2007

3.4.1 Experimental set-up

In the experiments carried out from 14 to 17 October 2007 all measurement techniques – TDL, lidar and micrometeorological mass balance method – were used to measure the emission from a manured circular plot.

Manure was applied onto the circular plot with a diameter of about 33 m on bare arable land. Normally, WUR uses plots of 50 m in diameter for the micrometeorological mass balance method. A relatively small plot was manured, so that the lidar would be able to measure the complete emission plume.

The circular plot was created by applying the manure over a pre-marked area in parallel passes that varied in length (see also Figure 2-11). The amount of manure applied to the plot was measured by weighing the manure tank before and after application. After application the manured area was measured by measuring the length and the width of the passes. The plot area was 856 m^2. The manure was surface applied. Surface spreading was carried out by a tanker fitted with a shallow injector. The shallow injector had a working width of 6.4 m and was kept about 10 cm above the soil while applying the manure. In combination with the high application rates in this experiment a situation of surface spreading was achieved. The application rate was 41.8 m^3 ha^{-1}. This high application rate was applied to achieve high volatilization rates in this experiment. Pig manure was applied, which was imported from pig farms by a contractor. Two manure samples were taken while the tanker was applying the manure onto the field. The manure was afterwards analysed for pH, dry matter and TAN content. On average, the pig manure contained 3.83 g TAN and 59.4 g dry matter per kg, and had a pH of 7.8.

As on 18 October, measurements started before the manure was applied. The application started on 9:48 and was finished on 9:52 UTC.

The micrometeorological mass balance equipment was left in place, measuring for 71 hours after manure application. The mast was placed in the centre of the plot, and a second mast at the windward (in this experiment: western) boundary of the manured plot. The central mast was placed there almost immediately after manure application had taken place on half of the plot.

The mobile lidar was sited to the southeast of the manured plot and measured northwards. The lidar measured continuously until the end of the next day.

The TDL measurements were carried out during the rest of the day, and resumed on the following day. The TDL and a wet chemical fast response denuder were driven up and down over a concrete farm

track to the east of the field. Next to this track, an Amanda wet annular denuder was placed. This instrument could be used while driving but had a significantly smaller response time than the Airrmonia used in the previous experiment. The data were used for calibration purpose of the TDL. Again gas bag samples were used for the intercalibration, and the two systems were operated next to each other a number of times. The fast response sensor data showed a significant tailing and was not used for emission evaluation. The TDLs were equipped with a short (1 m) inlet at the window in the middle of the car facing the manured circle (at the upwind side of the car). The car could drive backwards in this case so the orientation of the inlet with respect to the wind direction did not alternate when driving back and forth, which had been the case in the previous experiment.

For the Gaussian model z_o=0.1 and stability Pasquill class C were used. At these model settings the crosswind dispersion showed a good agreement with both the N_2O and NH_3 plumes. Five subsequent gas flask releases were used for the final correction of the dispersion model result. In this experiment, the distance of the circle to the measurement track was significantly smaller compared to the first manured circle experiment. The N_2O release was positioned behind the manure circle. This which implied that the N_2O plumes had a longer travel distance and therefore an extra dispersion. This effect could be evaluated with the model and was found to be 40%. This effect was taken into account with the correction obtained from the N_2O measurement.

No less than three wind measurement masts were present: the single solid-state wind meter from ECN, the mast with three solid-state wind meters from RIVM, and a mast with five cup anemometers plus a single wind vane from WUR. All were sited close to the manured section. See Figure 3-13 for an overview of the situation.

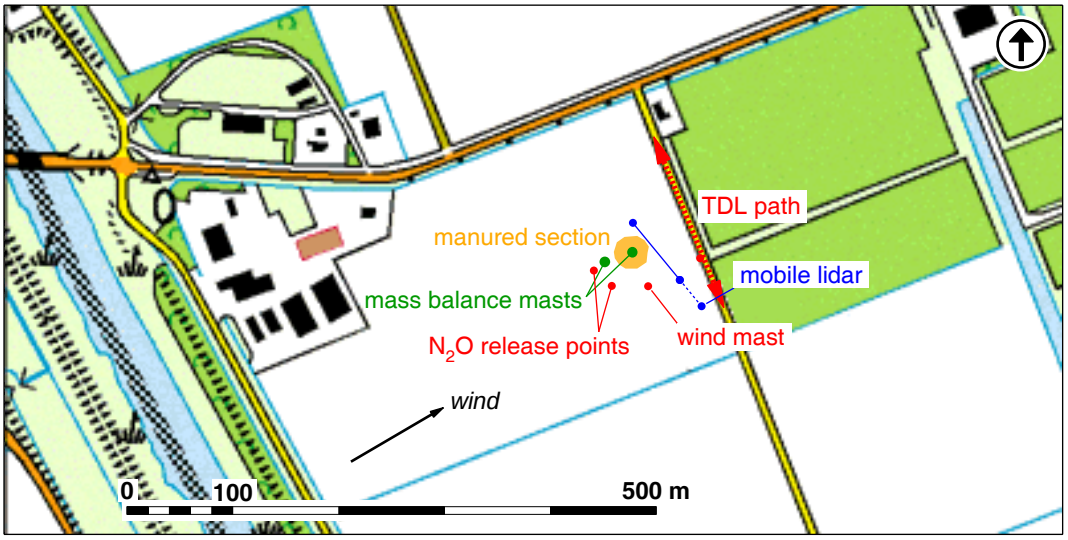

Figure 3-13. Oostwaardhoeve, the situation on 14 to 17 March 2007.

3.4.2 Measurement results

Meteorological conditions

The wind measurements taken these days are shown in Figure 3-14 and Figure 3-15, the latter zooming in on the two first measurement days.

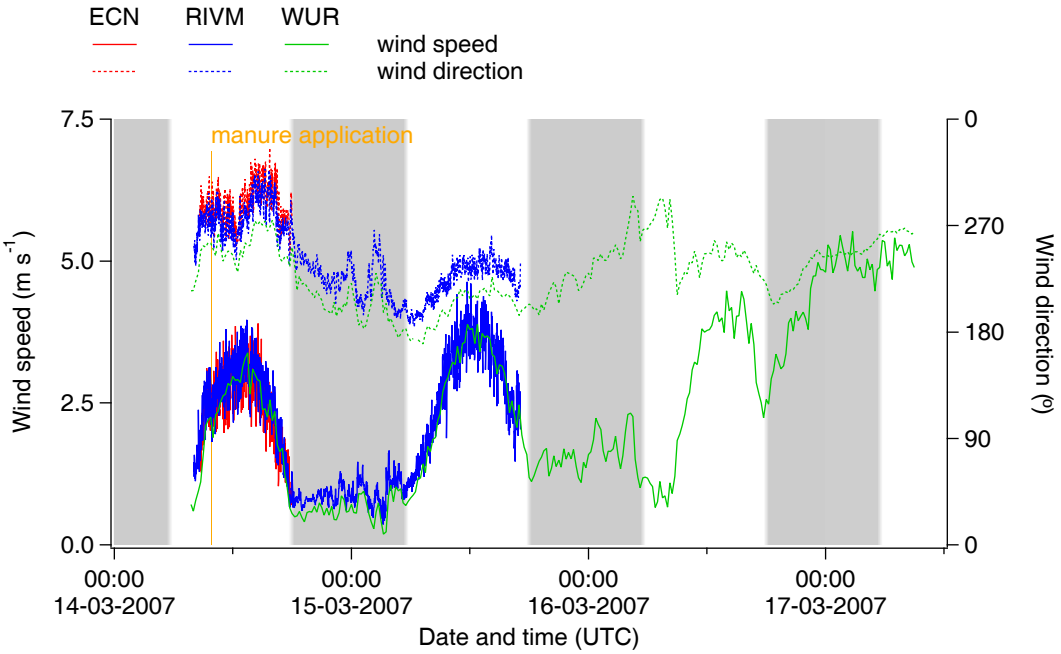

Figure 3-14. Oostwaardhoeve, wind speed and wind direction on 14 to 17 March 2007.

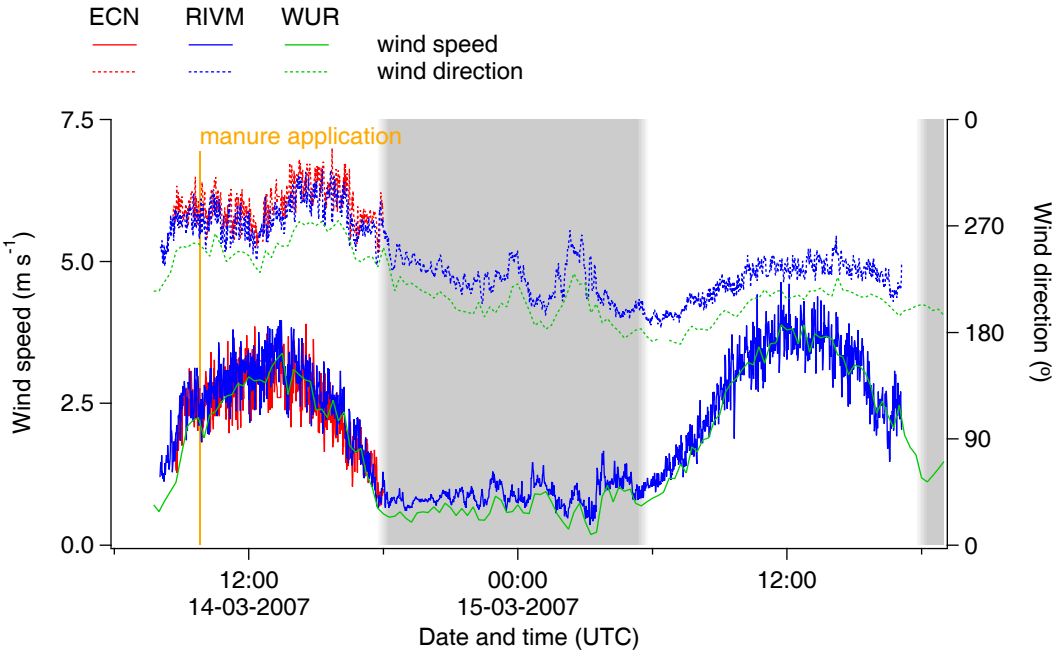

Figure 3-15. Oostwaardhoeve, wind speed and wind direction, zooming in on the period of 14 and 15 March 2007.

Concentration and emission measurements

Figure 3-16 shows the emission rate and cumulative emissions for the entire experimental period of 71 hours. Figure 3-17 and Figure 3-18 zoom in on the first two days and the first day of the measurements, respectively. On this day, 100% TAN corresponds to 160 kg NH_3-N ha^{-1}.

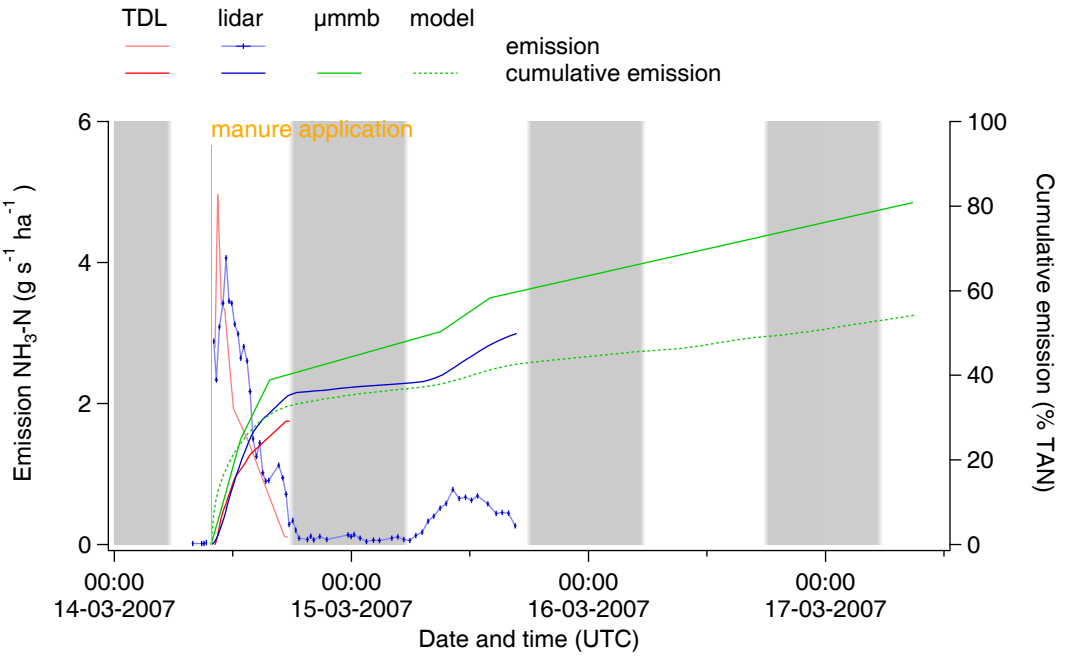

Figure 3-16. Oostwaardhoeve, graph showing the nitrogen emission (left axis) and the cumulative nitrogen emission (right axis) on 14 to 17 March 2007. µmmb: micrometeorological mass balance method.

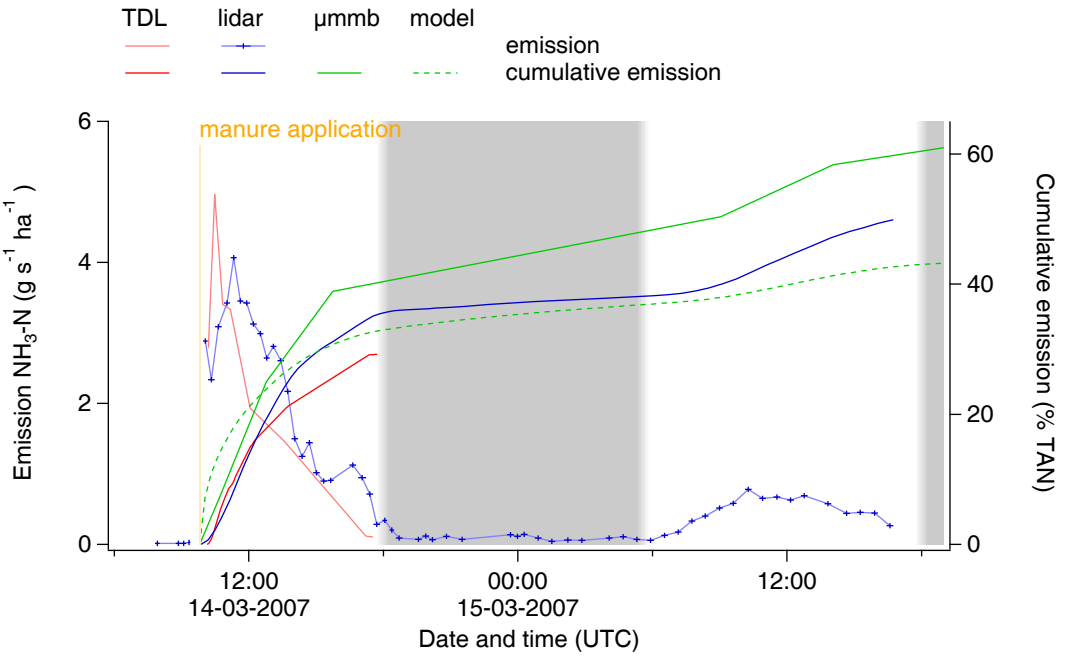

Figure 3-17. Oostwaardhoeve, graph showing the nitrogen emission (left axis) and the cumulative nitrogen emission (right axis), zooming in on the period of 14 and 15 March 2007. µmmb: micrometeorological mass balance method.

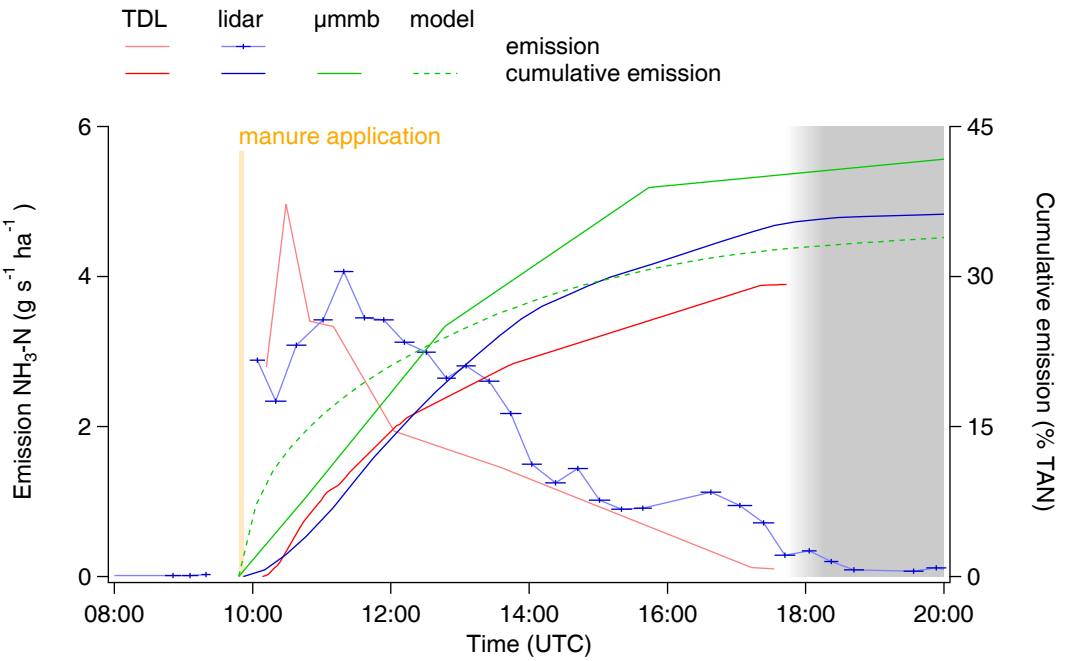

Figure 3-18. Oostwaardhoeve, graph showing the nitrogen emission (left axis) and the cumulative nitrogen emission (right axis), zooming in on 14 March 2007. µmmb: micrometeorological mass balance method.

3.4.3 Discussion

All three instruments show good agreement. The only deviation is the wind direction as reported by WUR, which is 20° further to the south than those measured by ECN and RIVM.

On 14 March, the TDL performed satisfactory. The difference in emission with changing direction of the car did not show in this data set. Calibration was easier to do. At the end of March 14, the instrument was stopped, to return the next day. On March 15 however, technical difficulties arose, precluding any additional measurements.

Throughout the first day, the lidar met with no particular difficulties. During the night, the wind speed diminished to values below 1 m s^{-1} (Figure 3-15). This is reflected in the very low emissions seen during that night; there was hardly any wind to carry the NH_3, if any, through the measurement plane. The next day, the measured emission increased again. Overnight, the wind had turned some 60° towards the south. This moved the emission plume towards the edge of the measurement range, which will lead to a slight underestimation of the emission.

The data collected on this day was also used to make an estimate of the precision of the lidar instrument when determining emissions. To do this, three measured data points were selected and re-analysed. In the regular analysis, ten vertical slices measured consecutively are averaged and analysed as a whole, to yield a single data point; for this exercise, the individual slices were analysed.

The data points selected were a background measurement, collected before manure application had started; the fourth data point after application, when the emission was peaking; and the 20th data point after application, when the emission had diminished considerably. The results are listed in Table 3-3.

Table 3-3. Lidar precision estimate.

measurement	average emission (g NH_3 s^{-1})	σ (g NH_3 s^{-1})	σ (%)
background	0.021	0.001	29
high emission	0.406	0.090	22
lowered emission	0.113	0.021	19

The mass balance measurements could be carried out as planned. The second day a measurement interval was set in line with a new lidar measurement set. Changes in wind direction have no influence on the measurements with the mass balance method. Although the wind speed was low during the night, still a good wind profile and concentration profile could be measurement and emission during the night could be calculated.

Figure 3-18 shows the measurement results for the first day. The emission measured by the lidar had its maximum some 1.5 hours after manure spreading had ended. This same behaviour was seen during the previous experiment, in October 2006 (see section 3.3). Contrary to the October experiment, this time the TDL measurements showed a similar pattern: the highest emission occurred 30 minutes after the end of manure spreading. The decline in emission during the rest of the day was seen by both instruments.

For the cumulative emission measurements, all three measurement methods coincided, with the mass balance measurements being some 16% higher, but following the same trend as the others. The TDL and the lidar came very close to the modelled cumulative emission, differing less than 5% from each other, and from the modelled emission.

The next day (Figure 3-17), there were no TDL measurements. The mass balance cumulative emission deviated further from that of the lidar, indicating that the lidar might have missed some emission during the night. The lidar measurement, in its turn, started to deviate from the modelled emission. Both measured curves showed the same shape: a significant emission was found during the second day, in the order of 33% (lidar) and 30% (mass balance) of the emission measured on the first day. The modelled emission only showed an increase of 18% on the second day. This significant emission during the second day was also found on the first experiment, in October.

3.5 Manured field – Oostwaardhoeve, 27 March 2007

3.5.1 Experimental set-up

This experiment took place on the same field on the Oostwaardhoeve, on 27 March 2007. This time, the manure was applied to the entire field; see Figure 3-19 for an overview of the situation. Manure application (Figure 3-20) started in the morning at 7:35 and continued until 12:22 UTC. Application started in the south-western corner of the field and was done in strips running parallel to the western edge of the field. Manure was applied by a tanker fitted with a shallow injector for grassland that applied the manure on top of the soil with hardly cutting a slot into the soil. The shallow injector had a working width of 6.4 m. Manure was applied on a total area of $94.5 \cdot 10^3$ m^2, the average application rate was 30.9 m^3 ha^{-1}. The application rate was estimated by counting the number of truck loads and from a delivery certificate of the contractor. Pig manure was applied, which was imported from pig farms by this contractor. Two manure samples were taken by WUR while the tanker was applying the

manure on the field. These samples were afterwards analysed for pH, dry matter and TAN content. On average, the pig manure contained 3.98 g TAN and 53.8 g dry matter per kg, and had a pH of 8.0.

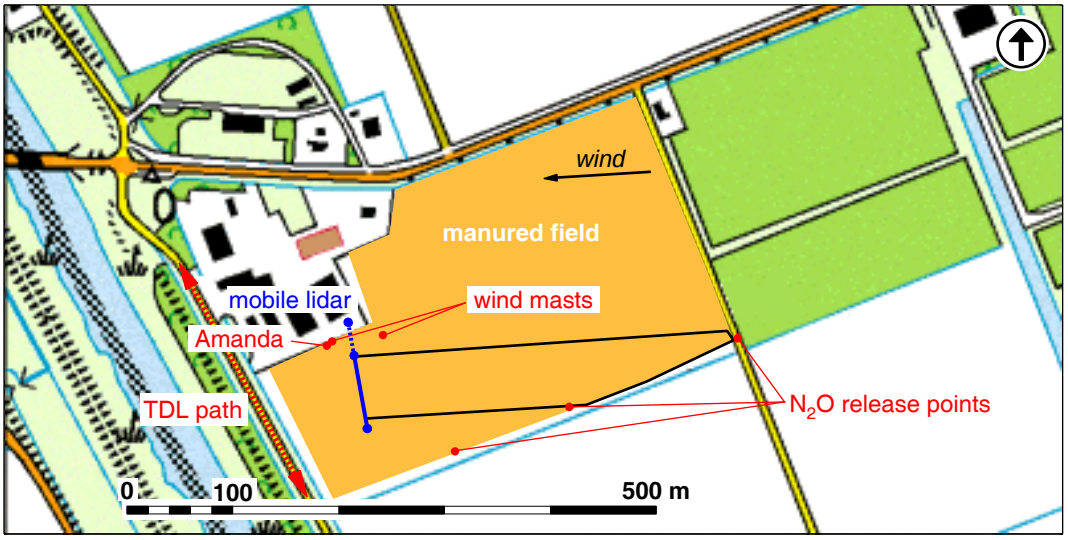

Figure 3-19. Oostwaardhoeve, the situation on 27 March 2007.

Figure 3-20. Manure application on the Oostwaardhoeve, 27 March 2007.

Measurements started before the manure was applied. The application was finished on 12:22 UTC. Measurements continued until the end of the day. Available instruments were the mobile TDL, the N_2O release system, an Amanda, the mobile lidar and the wind meters from ECN and RIVM. The mobile lidar was sited near the north-western corner of the field. The TDL was driven up and down the public road running to the west of the field. The Amanda and the wind meters were positioned near the mobile lidar. The Amanda data could not be used and calibration on this day had to rely on experiments performed the day before.

The evaluation of the data from this experiment is difficult compared to the previous experiments because of the fact that the manure application lasted all morning from 7:35 until 12:22. This implies that the total emission is gradually increasing to a maximum level over this episode with possible peaks in the emission whenever a new line on the field is manured. In the Gaussian model calculations, nine manure lines were used to simulate the emission. This pattern is shown in Figure 3-21.

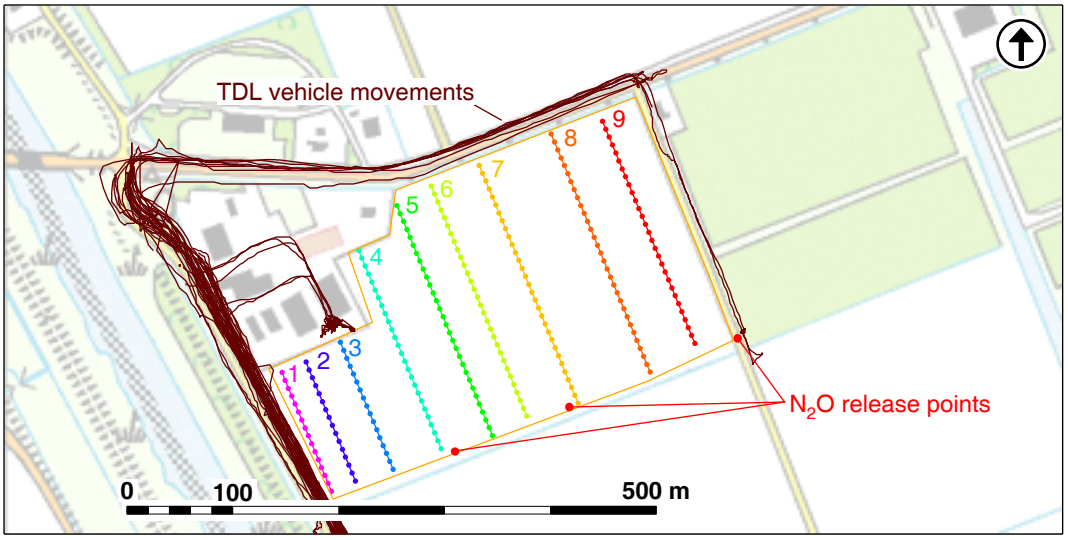

Figure 3-21. The nine lines on the field that were switched on subsequently in the model calculation, marked as 1 to 9; see also Figure 3-19.

Table 3-4 . Manuring time per line as used in the model. These times are start times for manuring the area around each line. For example, manuring the 2 ha around line 9 lasted from about 11:26 to 12:22.

line no.	time	area (ha)
1	7:35	0.244
2	7:49	0.244
3	8:03	0.390
4	8:32	0.812
5	9:01	0.942
6	9:30	0.707
7	9:59	0.975
8	10:43	1.462
9	11:26	2.161

For each line, the emission is assumed to be at a maximum at the start after which a decay sets in which will depend on wind speed, temperature and available TAN. No a priori assumptions were made on this temporal decay. Instead, the emission of each line was calculated using:

$$Q(t) = Q_o \cdot e^{-k\cdot(t-t_m)}$$ Equation 18

with Q_o = 1 g NH_3 ha^{-1} s^{-1}, t the actual time (for $t > t_m$), and t_m the time of manuring. For each line the Gaussian plume model was used to calculate the dilution/dispersion factor from the point sources on the line (as shown in Figure 3-21) to the actual position of the measurement van. The total concentration estimate with the model was calculated as the sum of the contributions of the nine individual lines.

The N_2O release system was placed at the southern edge of the field (Figure 3-19 and Figure 3-21). The model settings for z_o=0.1 and stability class C (slightly unstable) were calibrated using the N_2O tracer emission obtained in the afternoon. This had a ratio measured/modelled of 1 ± 0.4.

3.5.2 Measurement results

Meteorological conditions

The wind measurements taken these days are shown in Figure 3-22. The wind speed varied greatly during the day, but the wind direction stayed largely constant. The instruments are in good agreement on the wind speed, but differ in direction by some 25°.

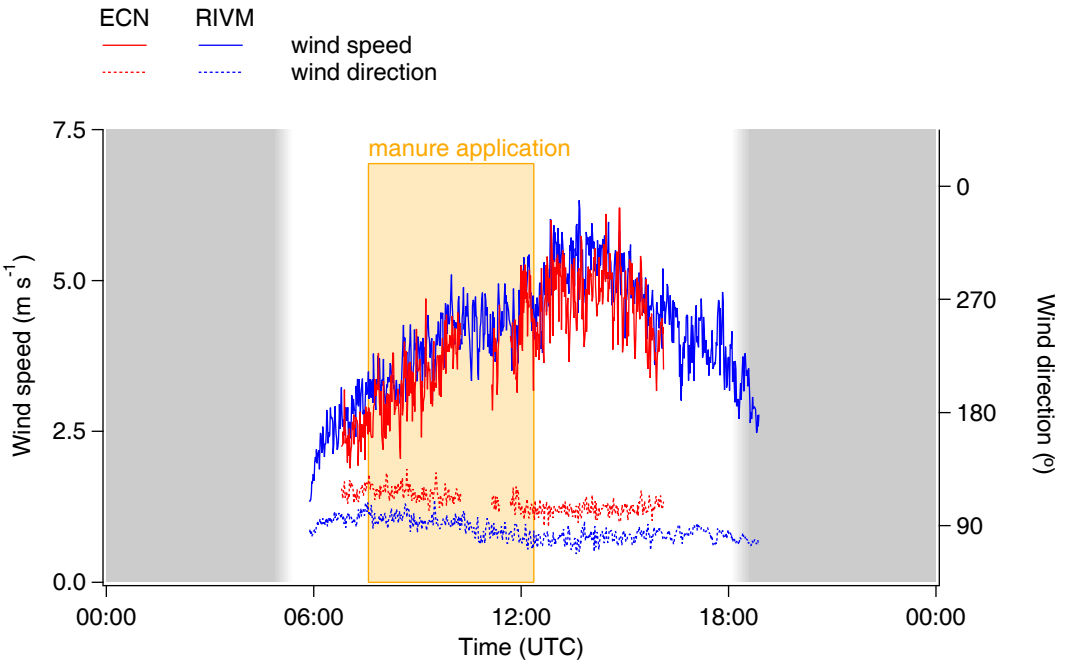

Figure 3-22. Oostwaardhoeve, wind speed and wind direction on 27 March 2007.

Concentration and emission measurements: TDL

The emission estimates from the TDL are shown in Figure 3-23. The emission estimates reflect the increase of the manured area. Depending on the choice of the decay constant k (see above) different emission estimates are obtained. The difference between those estimates increased at the end of the day.

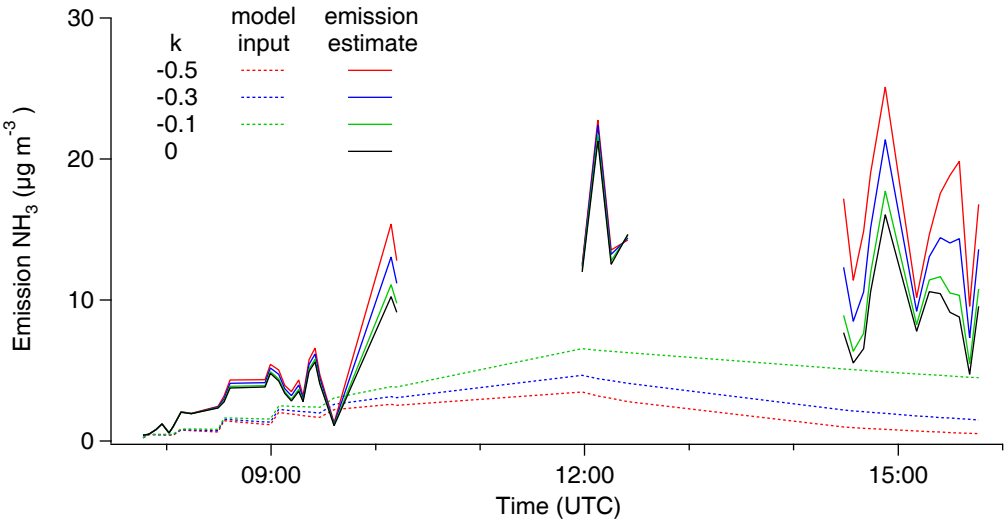

Figure 3-23. The emission put in the model as a function of time (dashed lines) and the resulting estimated emission for the field (solid lines), for 27 March 2007. Shown for different assumed k factors.

In Figure 3-23 the effect of the choice of k is demonstrated. With k = -0.5 the emission assumed in the model decreases rapidly and the modelled concentration levels decrease as well. Since the estimated emission is obtained from measured divided by modelled concentration plumes, the emission estimate will be relatively high at the end of the day. With k = -0.1 the assumed emission in the model at the end of the day is higher and thus a lower emission estimate is obtained.

During the manuring episode, the decay in the emission from the first lines will be compensated for by the increasing area that is manured. After manuring of the whole field, all lines will show a decay in emission according to the formula given in Equation 18. Therefore the level of k can be determined in this episode. At the best value for k both measured and modelled concentration levels in the plume will decay with the same speed. This implies that the ratio between measured and modelled plume integrals should become constant. Table 3-5 shows the average of the ratio for three sets of three to five plumes, each around 12:11, 14:30 and 15:30. The ratio between measured and modelled plume integrals is shown for the range of k between -0.5 and 0 h^{-1}. A clear minimum in the standard deviation (7%) of these three values is obtained at k = -0.1 h^{-1}. For k = -0.2 and k = -0.05, this standard deviation is 16% respectively 19%. These two levels were used to assess the uncertainty in the cumulative emission estimate over the whole measurement episode.

In Figure 3-24 the emission is again shown in g N ha^{-1} s^{-1}, which shows a rather constant emission during the morning. In the afternoon a decay also is shown in the per hectare emission. The lower half of the graph shows the estimated total emission in kg N ha^{-1} which ranges from 38 for k = -0.2 to 41 at k = -0.05. Most likely value is 39 at k = -0.1.

Table 3-5. The ratio between emission input in the model and final emission estimate obtained for different k-factors.

decay factor k	-0.5	-0.3	-0.2	-0.1	-0.05	0
time			**ratio measured/modelled emission**			
12:11:33	5.08	3.58	2.95	2.39	2.14	1.90
14:39:58	19.63	6.61	3.76	2.11	1.57	1.17
15:29:17	25.79	7.59	4.03	2.12	1.53	1.10
relative standard deviation	63%	35%	16%	**7%**	19%	32%

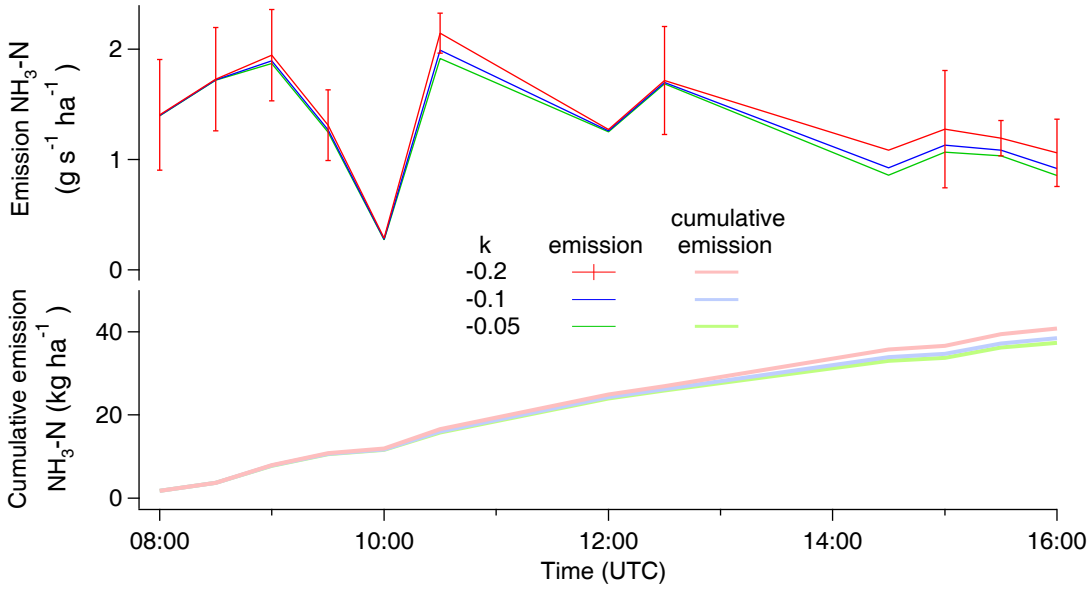

Figure 3-24. Emission level in g N ha^{-1} s^{-1} (upper part) and cumulative level in kg N ha^{-1} (lower part) er 30 minute interval, for 27 March 2007. Error bars indicate the standard deviation of the different estimates in each 30 minute interval. At 10:00, 12:00 and 14:30 only one estimate is available.

Concentration and emission measurements: lidar

In contrast with the previous experiments, not the entire emitted plume is visible in the lidar measurements. This means that an estimate must be made: the NH_3 that is measured, which part of the surface emitted it? As a first guess, it was assumed that only the surface straight upwind from the measurement interval contributed to the NH_3 measured. This surface is depicted in Figure 3-19, as a black polygon.

Manure spreading spanned a period of almost five hours. During this period, the emitting surface steadily increased. The location of the applicator was not precisely logged during this experiment. Therefore, to make an estimate of the development of the emitting surface over time, this surface was linearly interpolated between 0 ha at the start of the application, and 1.84 ha (the area of the black polygon in Figure 3-19) at the end.

A more sophisticated approach would take into account the fanning out of the ammonia plume emitted from the surface, as is done with the Gaussian dispersion model (see above). Due to this fanning, a plume originating within the area directly upwind will stretch out beyond the borders of the measurement plane. However, a plume coming from outside that area will stretch out to within those borders. For these experiments, the two effects cancel each other out on the northern edge of the upwind area. On the southern edge this is not the case, because there the edge almost coincides with the edge of the field. The simple approach outlined above is thus expected to lead to an underestimation of the determined emission. Taking into account this fanning out would require knowledge of the extend to which the plumes spread, the rate with which the emission declines (see above), and the precise moments at which the manure was applied to each part of the field. Unfortunately, that data is not available. So far, no attempt was made to take this effect into account.

Figure 3-25 shows the emission rate and cumulative emissions for this day both for the TDL and for the lidar. On this day, 100% TAN corresponds to 123 kg NH_3-N ha^{-1}.

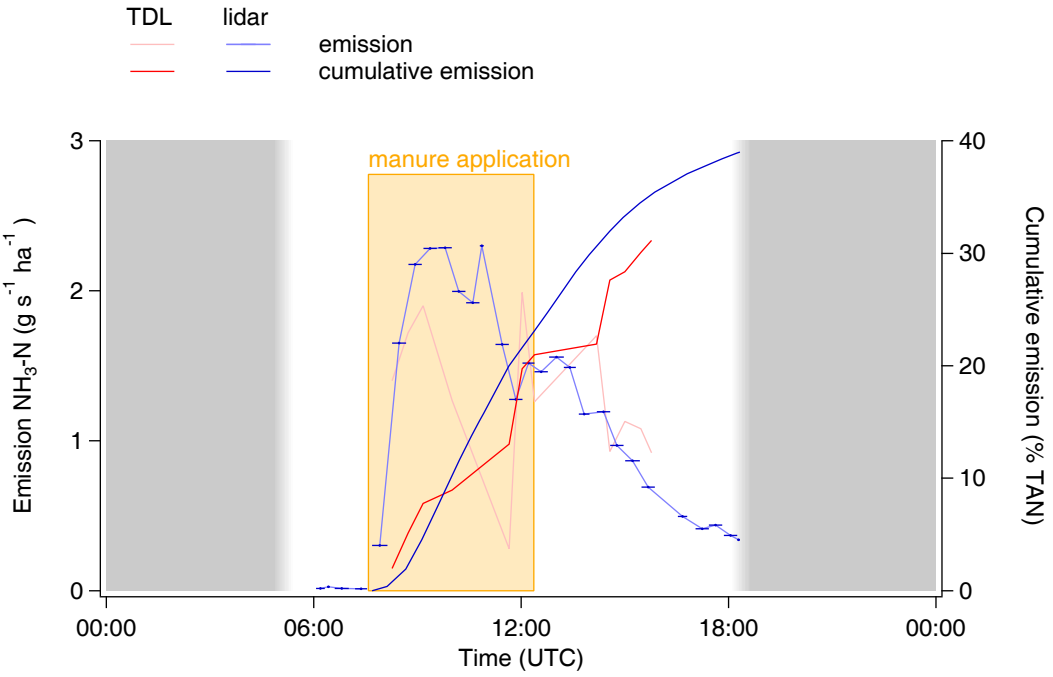

Figure 3-25. Oostwaardhoeve, graph showing the nitrogen emission rate (left axis) and the cumulative nitrogen emission (right axis) on 27 March 2007.

3.5.3 Discussion

The main complicating factor in the interpretation of this experiment is the long time – almost five hours – it took to apply the manure.

When the workaround described above is used, the lidar measurements report a cumulative emission of 39% of the TAN. Because of the difficulties associated with the determination of the emitting surface, this data should be used with care.

For the TDL measurements the conclusion is that plume measurements can be used for full field emission analyses. The decay function for the factor k can be derived from the emission measurements

as soon as the whole field is manured. The uncertainty in the final emission related with this k factor is relatively small (10%). The per hectare emission level was relatively constant during the morning and decreased in the afternoon. Apparently the decay in the emission in the fist lines was almost compensated for by the extra emission in subsequent lines that were manured. The per hectare emission at 10:00 in the morning seems very low (based on one data point) and it might be better to reject this data point. This was not done, because for the net cumulative emission, the effect is small (38 kg N ha^{-1} instead of 39 kg N ha^{-1} after rejection).

3.6 Manured field 1 – Woerden, 3 August 2007

3.6.1 Experimental set-up

In August 2007, three experiments were carried out on the commercial dairy farm in Woerden. The map in Figure 3-26 shows the locations of the fields that were manured during these days. Figure 3-27, Figure 3-36 and Figure 3-39 show the situations in more detail.

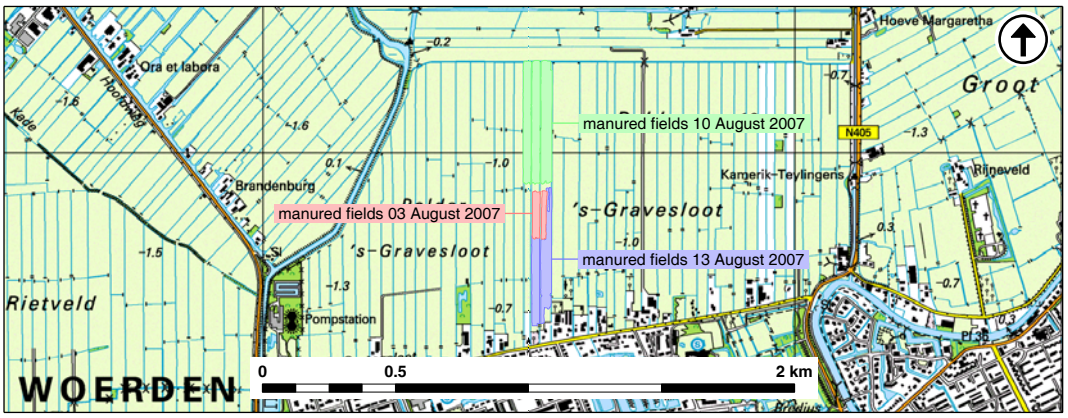

Figure 3-26. Woerden, locations of the manured fields, August 2007.

On 3 August 2007, emissions were measured from two manured field sections. For farming operational reasons, not the entire fields were manured. However, the sections manured were large compared to the measurement range of the mobile lidar, so that for this instrument the experiment can be classified as being done on a whole-field scale.

Manure application started at 08:03 and continued until 09:06 UTC. A total of $27 \cdot 10^3$ kg of manure was applied by the dairy farmer with a tanker fitted with a shallow injector for grassland. This injector applied the manure on top of the soil while hardly cutting a slot into the grass sod, creating the work result of the trailing foot application technique. The working width of the applicator was 6 m. The tractor pulling the tanker was equipped with a hand-held GPS (Garmin, GPSmap 60CSx) that logged the tractor's position every two seconds, to track the manure spreading pattern. Manure was applied on a total area of $8 \cdot 10^3$ m^2. The average application rate was 33.5 m^3 ha^{-1}.

The application rate was estimated by counting the number of tank loads applied. A mixture of dairy and pig manure was applied. The dairy manure was produced by the cows at the farm, the pig manure

was brought in from other farms. Four manure samples were taken while the tanker was applying the manure onto the field. These samples were afterwards analysed for pH, dry matter and TAN content. On average, the dairy manure contained 2.74 g TAN and 59.3 g dry matter per kg, and had a pH of 7.5. After manure application, the perimeter of the manured fields was walked with the above-mentioned GPS in hand, to map the extend of the manured section.

Present were the mobile TDL, the N_2O release system, an Amanda, the mobile lidar and the wind meters from ECN and RIVM. WUR took manure samples. All instruments started measuring before manure application started, and continued to do so until the end of the day.

The mobile lidar was sited to the east of the field and measured due north. The TDL was driven up and down a metalled farm track running from south to north to the east of the field (Figure 3-28). The Amanda (Figure 3-30) was positioned next to the mobile lidar scanning plane. The wind meters were positioned in an un-manured part of the field. The N_2O release system was placed between the two manured field sections. See Figure 3-27 for an overview of the situation.

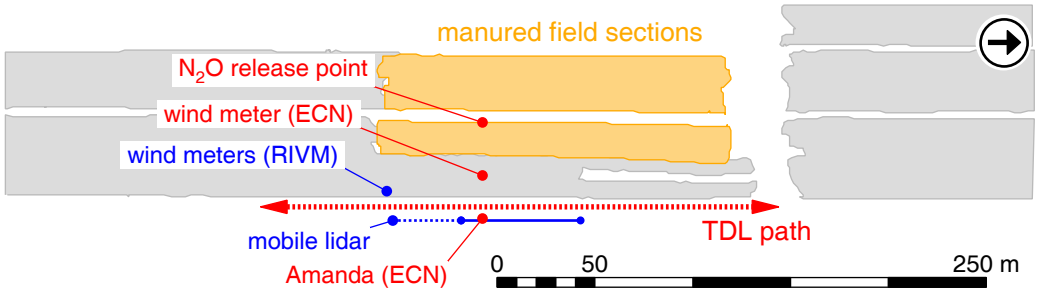

Figure 3-27. Woerden, the situation on 3 August 2007.

Figure 3-28. The TDL and the lidar in Woerden, 3 August 2008.

The N_2O release system vented N_2O at a rate of 0.14 g s^{-1}. The N_2O concentration measurements were done to evaluate the plumes that originated from this tracer release system. The emission of N_2O from the manured fields itself was not large enough to be evaluated with these measurements. This was checked before starting the release system. The Amanda measurement was operated with a flow through the wet annular denuder of 30 L min^{-1}. Concentration calibrations were performed in the field using standard NH_4^+ solutions to cover the range from 0 to 1000 µg NH_3 m^{-3}. Calibration of the TDL using the Amanda was done using a gas mixing system in which ambient air was mixed with air bubbled through a concentrated aqueous ammonia solution. The system delivered air at a rate of 40 L min^{-1} that had an NH_3 concentration of 500 ± 20 µg m^{-3} higher than the concentration in ambient air. It was also used to evaluate the response time of the TDL and the Amanda set-ups. These were 2 s and 3 min, respectively, for the 500 µg m^{-3} step in the concentration.

The Amanda system was used once on this day to measure a vertical NH_3 concentration profile. This was done by raising an 8 m inlet tube into the air (Figure 3-30) and measuring at a number of altitudes. Measurements were done in the afternoon when concentrations at 1.8 m height had decreased from 500 µg m^{-3} in the morning to about 200 µg m^{-3}.

Model runs for N_2O were performed using Pasquill stability C, z_o = 0.05 m and a release height of 1 m for the N_2O flask. For NH_3 the field was divided in nine lines. Each line consisted of eighteen point sources as shown in Figure 3-29. A model run using the 1 Hz meteorological data was done both for the Amanda location and for the position of the moving van. A second run was done using 15 minute averaged meteorological data.

The nine time series were all multiplied with the same temporal function:

$$Q(t) = Q_o \cdot e^{-k\cdot(t-t_{application})}$$ Equation 19

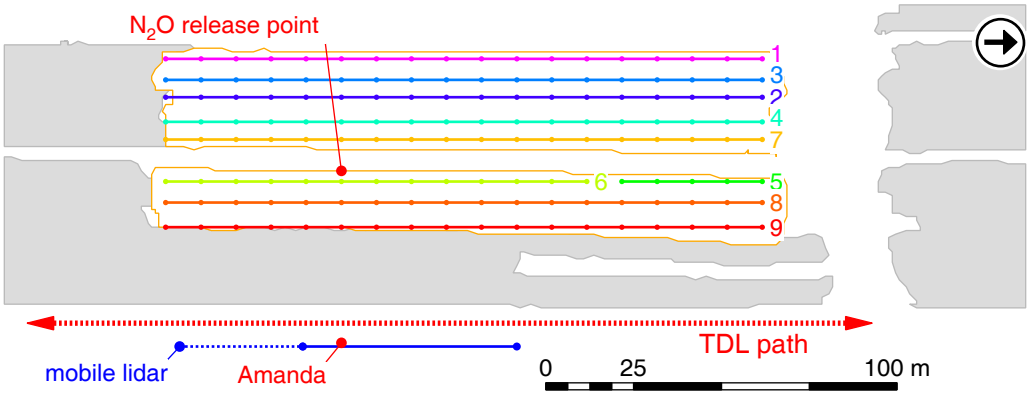

Figure 3-29. The nine lines on the field that were switched on subsequently in the model calculation, marked as 1 to 9; see also Figure 3-27. The wind was west, i.e. from top to bottom in this Figure.

Table 3-6. Emission lines and times used in the model.

line no.	start time	area	source
1	8:01	0.102	1.00
2	8:05	0.102	1.00
3	8:21	0.102	1.00
4	8:24	0.102	1.00
5	8:27	0.029	0.28
6	8:41	0.073	0.72
7	8:49	0.102	1.00
8	9:00	0.102	1.00
9	9:04	0.102	1.00

The nine time series were added to obtain the modelled concentration at the Amanda location.

Figure 3-30. TDL and Amanda measurement setup (left), Amanda wet annular denuder (middle), profile measurement (right).

3.6.2 Measurement results

Meteorological conditions

The wind measurements taken on this day are shown in Figure 3-31.

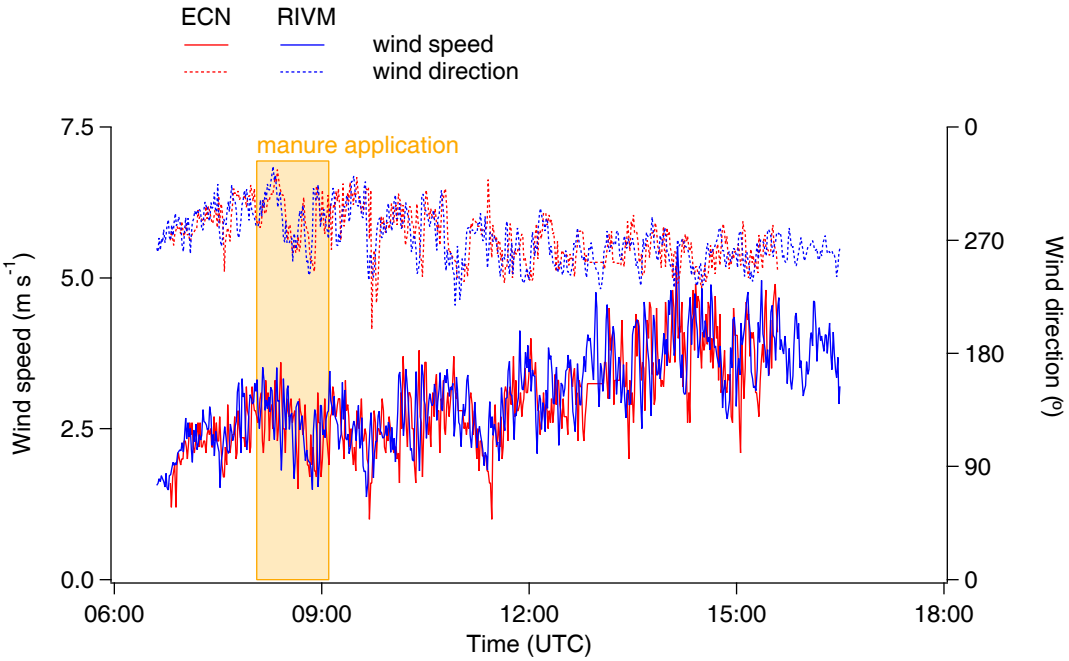

Figure 3-31. Woerden, wind speed and wind direction on 3 August 2007.

Concentration and emission measurements

An example of measured N_2O peaks from the gas flask release at 50 m upwind from the measurement transect is shown in Figure 3-32. Typical peak concentrations in the plume at 30-40 m distance were 1000 ppb which gave a signal-to-noise ratio of about 10.

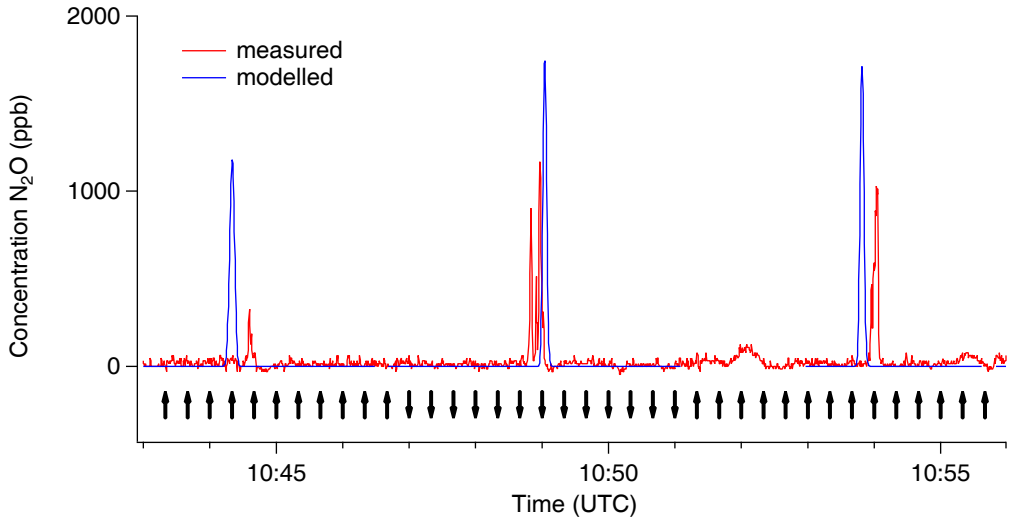

Figure 3-32. Example of the measured and modelled N_2O plumes. The row of arrows at the bottom indicates the direction of the movement of the vehicle.

The source strength estimated from the model plumes integrated along the measurement transects was 0.11 g N_2O s^{-1}, which is 19% below the true value of 0.13 g N_2O s^{-1} released. This factor was used to correct the emission factors obtained for the NH_3 plumes. With similar model settings (except for a release height of 0.1 m), NH_3 concentration patterns were evaluated using the nine different manured source lines on the field. In total, 43 plume transect measurements were obtained. The emission estimates were calculated using the ratio of the integrated measured and modelled NH_3 plumes.

The parameters Q_o and k were optimized using the episode after all manure was applied (after 9:30). This was done using the Microsoft Excel Solver tool which is based on the Generalized Reduced Gradient (GRG2) nonlinear optimization code developed by Leon Lasdon, University of Texas at Austin, and Allan Waren, Cleveland State University. A minimum in the difference between measured and modelled NH_3 concentration was obtained for Q_o = 1.81 g NH_3 s^{-1} and k = -0.110 $hour^{-1}$ (which is similar to the value obtained in the 27 March experiment at the Oostwaardhoeve). The resulting concentration pattern is shown in Figure 3-33. The time function in the model was fitted to the measurements for the episode after 9:30. For the episode when manure is being applied the function overestimates the concentration at the Amanda site. Apparently the emission at that time is below the modelled level. A corrected emission pattern was obtained using:

$$\text{Emission}_{\text{corrected}}(t) = \text{Emission}_{\text{model}}(t) \cdot \frac{C_{\text{measured}}}{C_{\text{modelled}}} \qquad \text{Equation 20}$$

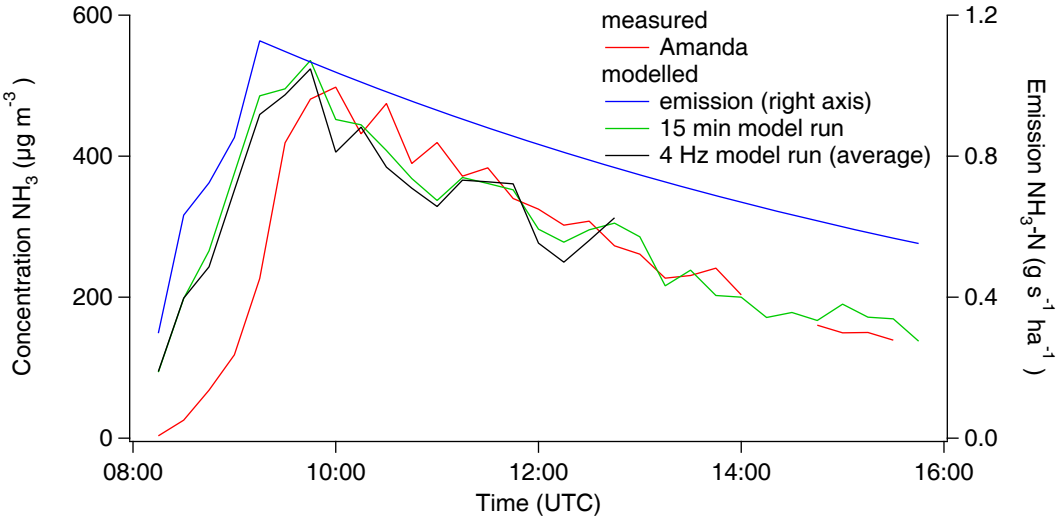

Figure 3-33. Initial model emission curve (blue) and the resulting concentration patterns modelled at the Amanda position. The Q_0 and k parameters were adjusted to provide the fit of the model to the decay in the NH_3 concentration after 9:30. Also shown is the concentration measured by the Amanda (red curve).

Vertical concentration profile measurement with the Amanda

From 14:00 to 14:30 UTC, a vertical concentration profile was measured with the Amanda; see Figure 3-34. At that time, the lidar measurements indicated that the edge of the plume was at a height of about 5 m. Indeed, the NH_3 concentration at 8 m was only about 30 µg m^{-3}, and the main increase in the concentration occurred when the inlet was lowered from 6 to 4 m. The concentration profile was also modelled. This showed similar results; see Figure 3-34. Apparently the model settings that were tuned for the N_2O plumes (with a focus on the horizontal dispersion) give a proper description of the vertical mixing.

The length of the inlet system caused an increase in the response time of the system. Going up from 1.8 to 8 m the system took 20 minutes to decrease in concentration from 250 to 30 µg m^{-3}. The lower concentrations obtained with the measurements as compared to the model run are probably related to this delay effect, caused by the long inlet tube.

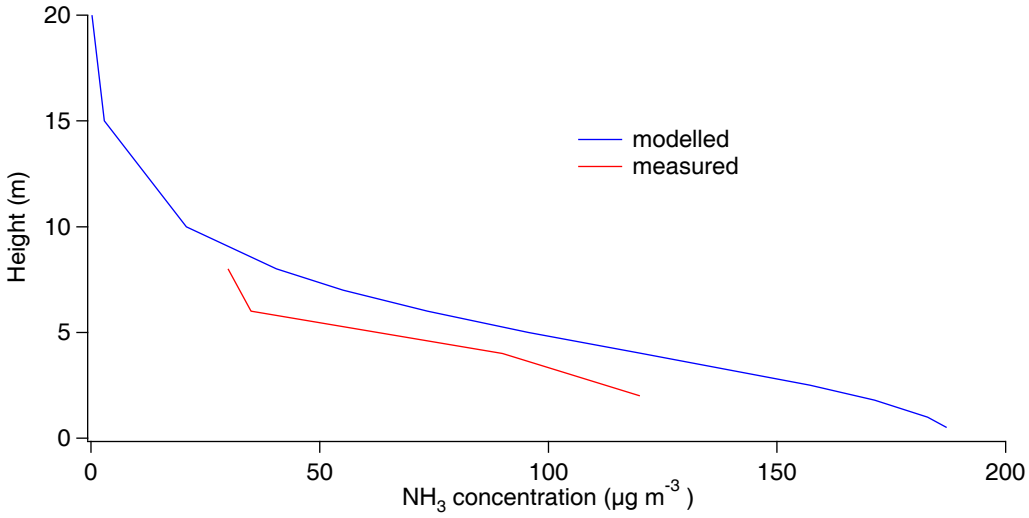

Figure 3-34. Modelled and measured vertical NH_3 concentration profile.

Figure 3-35 shows the emission rates and cumulative emissions obtained with the TDL, the Amanda and lidar for this day. On this day, 100% TAN corresponded to 83 kg NH_3-N ha^{-1}.

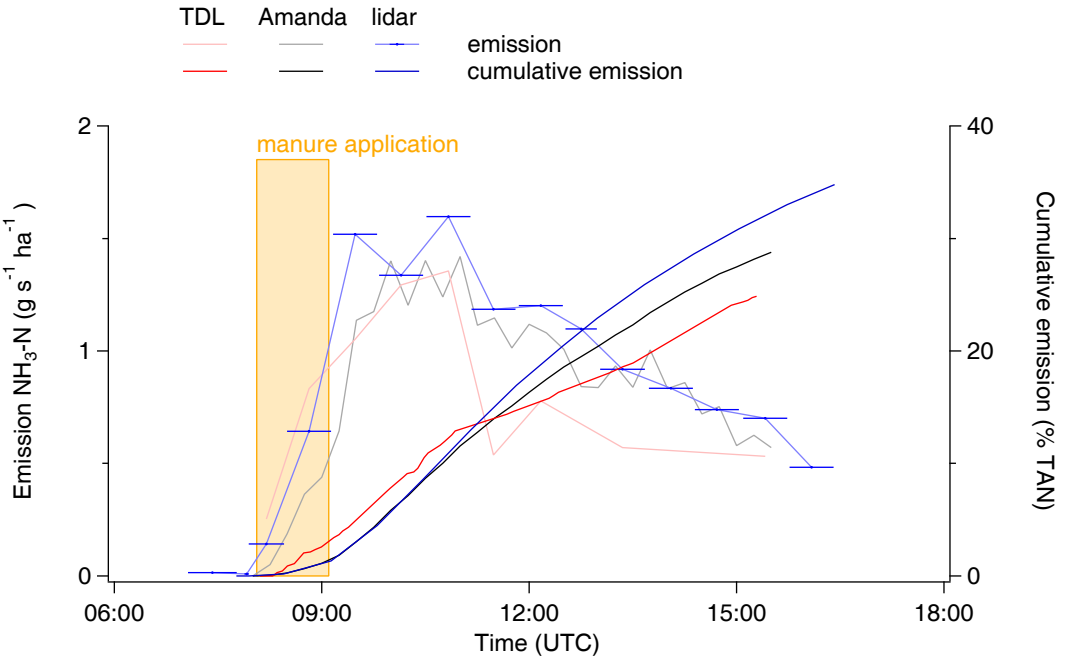

Figure 3-35. Woerden, graph showing the nitrogen emission (left axis) and the cumulative nitrogen emission (right axis) on 3 August 2007.

3.6.3 Discussion

Wind speed increased somewhat during the day, but the wind direction stayed largely constant. The instruments are in good agreement.

As with the previous experiment, not the entire emitted plume is visible in the lidar measurements. This time, defining an emitting surface is easier: because applying the manure took only one hour, the error introduced by not taking this period into account is much smaller. The fanning out, discussed in section 3.5.2, is expected not to play a role in this experiment. Here, as on the northern edge of the upwind surface at the Oostwaardhoeve, the fanning out of the plumes outside and inside the area directly upwind cancel each other out. Therefore, the emitting surface was taken as the manured surface straight upwind from the lidar measurement interval. The latter is indicated in Figure 3-27; it is the solid part of the blue line emanating from the dot marked as “mobile lidar”.

As observed in the two manured circle experiments at the Oostwaardhoeve, the emission maximum is two hours after the end of the manure application, then the decrease sets in.

The NH_3 emission as estimated from the TDL and Amanda measurements also shows an increase in the first 1.5 hours. The difference between the emission pattern as determined by the measurement at a single location with the Amanda and the whole plume transects obtained from the TDL is not fully understood at the moment. The initial higher peaks observed with the TDL setup could indicate an effect of inlet damping or saturation at the Amanda system. However, the response time that is observed when the bubbler system is connected is three to five minutes. In the afternoon the emission levels obtained from the Amanda data are above those obtained from the plume measurements. These estimates are probably better compared to those obtained with the TDL because it is clear that the uncertainty in the afternoon increases in the TDL plume emission measurement with low (about 2 to 3) signal-to-noise ratios.

In general the signal-to-noise ratio for the NH_3 measurements needs further improvement. A main problem is degradation of the mirrors in the multipass cell with dust entering the cell.

The bubbler system is an important improvement to obtain well-calibrated data from the TDL system.

Until 11:30, the emission rates reported by the TDL and the lidar are in good agreement. After that time, the rate measured by the TDL starts to diminish. As explained above, this is probably due to the low signal-to-noise ratio of the TDL concentration measurements. The emission rates measured by the Amanda and those measured by the lidar agree well, with the Amanda measuring slightly lower values (some 14%).

3.7 Manured field 2 – Woerden, 10 August 2007

3.7.1 Experimental set-up

On 10 August 2007, three fields were manured. Present to measure were only the mobile lidar, the RIVM wind meter mast, and WUR, to take manure samples. The mobile lidar and the wind mast were sited to the south-east of the manured fields. The lidar measured almost due west. See Figure 3-36 for an overview of the situation.

Manure application started at 9:59 and continued until 14:45 UTC. A total of $108 \cdot 10^3$ kg of manure was applied by the dairy farmer. The procedure of the application was the same as on 3 August (see section 3.6.1). Manure was applied on a total area of $46 \cdot 10^3$ m^2, the average application rate was 23.3 m^3 ha^{-1}. Four manure samples were taken while the tanker was applying the manure on the field.

These samples were afterwards analysed for pH, dry matter and TAN content. On average, the manure contained 2.47 g TAN and 61.2 g dry matter per kg, and had a pH of 7.5. After manure application, the perimeter of the manured fields was walked with the GPS in hand, to map the extend of the manured section.

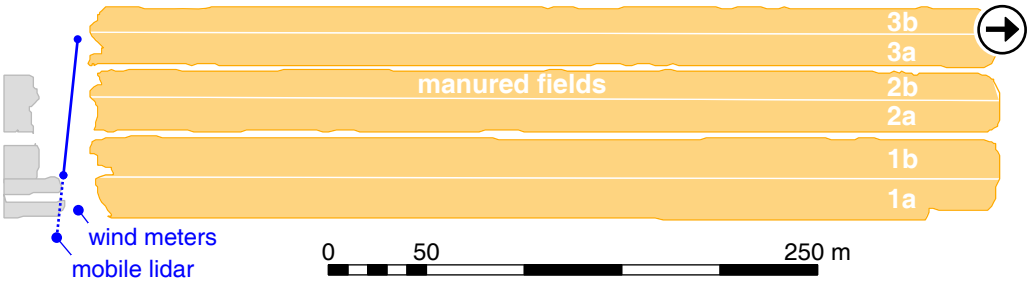

Figure 3-36. Woerden, the situation on 10 August 2007.

The lidar started measuring before manure application started, and continued until the end of the day.

3.7.2 Measurement results

Meteorological conditions

The wind measurements taken on this day are shown in Figure 3-31. Both wind speed and wind direction were fairly constant during the day.

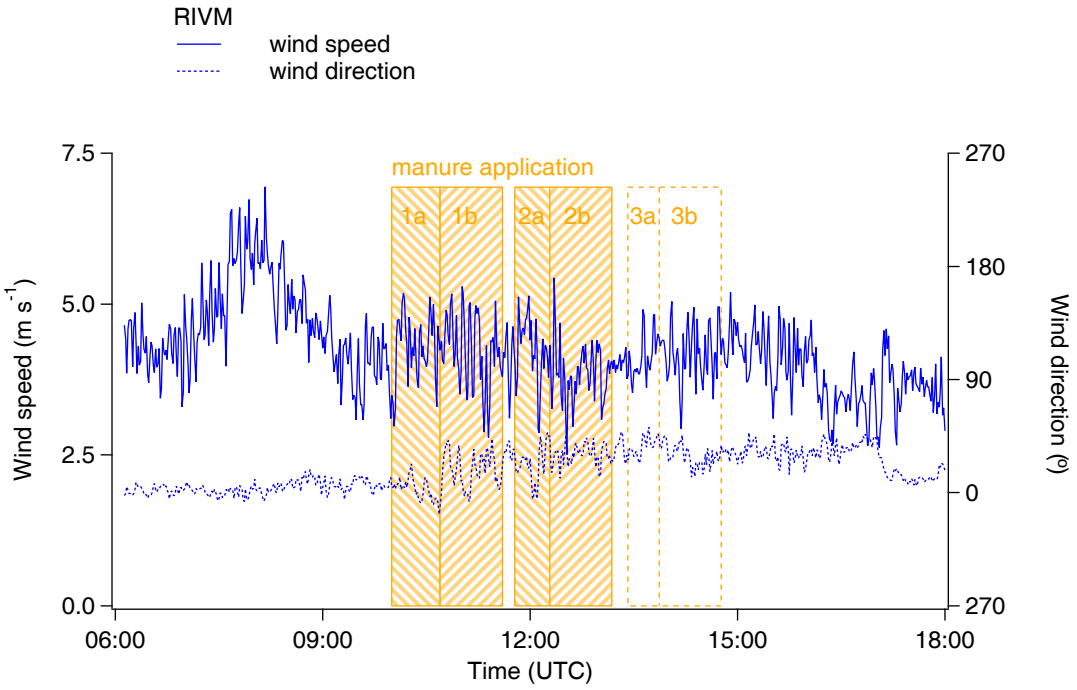

Figure 3-37. Woerden, wind speed and wind direction on 10 August 2007.

Concentration and emission measurements

Because the lidar measured almost due west, measurements had to be terminated earlier than expected, when the setting sun started to come close to the fields of view of the telescope and of the security camera.

Figure 3-38 shows the emission rates and cumulative emissions for this day. On this day, 100% TAN corresponds to 57 kg NH_3-N ha^{-1}. The manure application period is split up in six parts, each corresponding to a part of a field. These parts are indicated in Figure 3-36 as well.

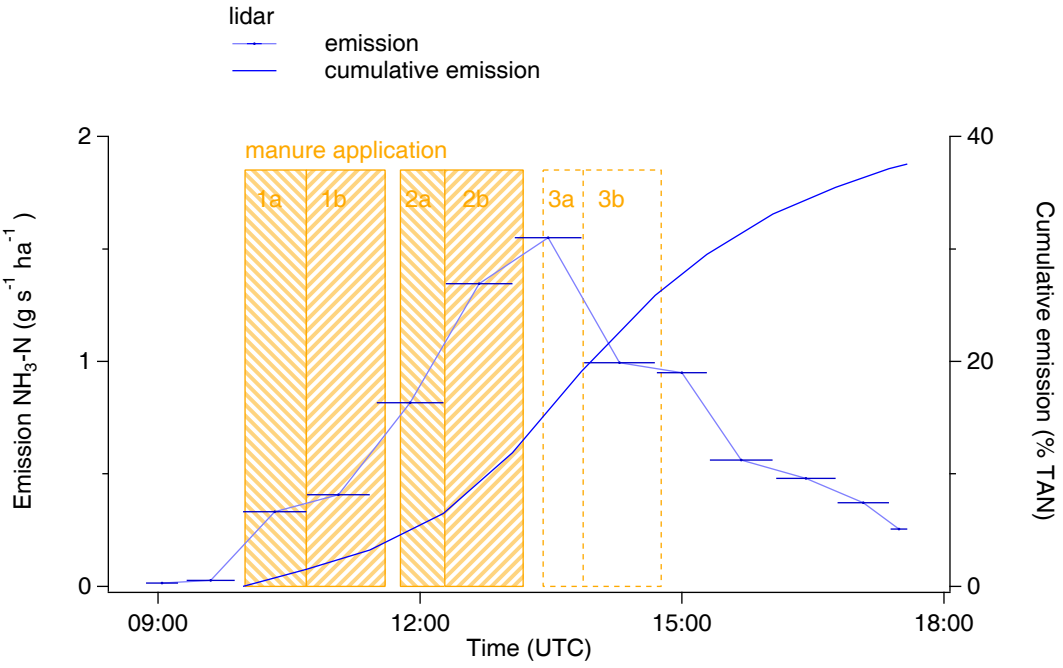

Figure 3-38. Woerden, graph showing the nitrogen emission (left axis) on 10 August 2007.

3.7.3 Discussion

Lidar measurements

On 10 August 2007, the wind blew almost straight from the north. The manured fields were elongated, and were oriented along a north-south axis (Figure 3-36). This means that the emitting surface determination is rather sensitive to even small variations in the wind direction. Unfortunately, there are such variations. To deal with them, the following procedure was adopted.

For a wind measurement taken, the average (over three wind meters) wind direction was calculated.

From this wind direction, a rectangle was drawn like the one depicted in Figure 3-19. Two of its corners coincided with the start and end of the lidar measurement range, the other two were situated 550 m upwind from the first two points.

If this rectangle overlapped with one or more field sections that had at that moment manure on them, the area of overlap was determined.

This process was repeated for each wind measurement taken.

For each lidar measurement period, denoted in Figure 3-38 with a horizontal line on the emission rate curve, the average emitting surface was determined from the areas of overlap for this period.

From this exercise, it turned out that field 3 did not contribute to the emitting surface until well in the afternoon; only the last two lidar measurements see ammonia from that field. Therefore, manure application can be considered finished after field 2.

Contrary to the earlier experiments, the maximum emission rate in this experiment was reached just after manure application had been finished. However, the decline that set in after the maximum was just as steady as observed in previous experiments.

These results suggest that the determination of the emitting surface. In conclusion, the findings for this day corroborate with those from the previous day, but should be used with care, because the emitting surface determination was complicated.

3.8 Manured field 3 – Woerden, 13 August 2007

3.8.1 Experimental set-up

On 10 August 2007, the remaining area of the fields from 3 August 2007 were manured. Present to measure were only the mobile lidar, the RIVM wind meter mast, and WUR, to take manure samples. The mobile lidar and the wind mast were sited to the east of the manured fields. The lidar measured to the northwest. See Figure 3-39 for an overview of the situation.

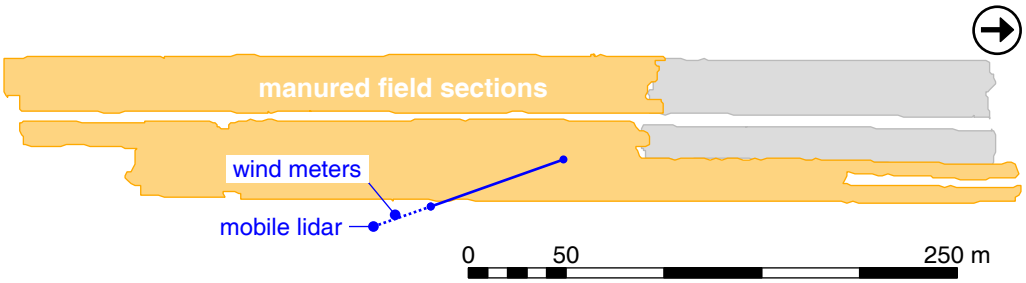

Figure 3-39. Woerden, the situation on 13 August 2007.

Manure application started at 8:03 and continued until 9:52. A total of $54 \cdot 10^3$ kg of manure was applied by the dairy farmer. The procedure of the application was the same as on 3 August (see section 3.6.1). Manure was applied on a total area of $24 \cdot 10^3$ m^2, the average application rate was 22.2 m^3 ha^{-1}. Four manure samples were taken while the tanker was applying the manure on the field. These samples were afterwards analysed for pH, dry matter and TAN content. On average, the manure contained 2.43 g TAN and 71.8 g dry matter per kg, and had a pH of 7.5. After manure application, the perimeter of the manured fields was walked with the GPS in hand, to map the extend of the manured section.

Lidar measurements started when manure application had already begun, and continued until the end of the day.

Figure 3-40. The lidar in the agricultural landscape just to the north of Woerden.

3.8.2 Measurement results

Meteorological conditions

The wind measurements taken these days are shown in Figure 3-41. The wind direction was fairly constant during the day, this facilitated the interpretation of the lidar measurements.

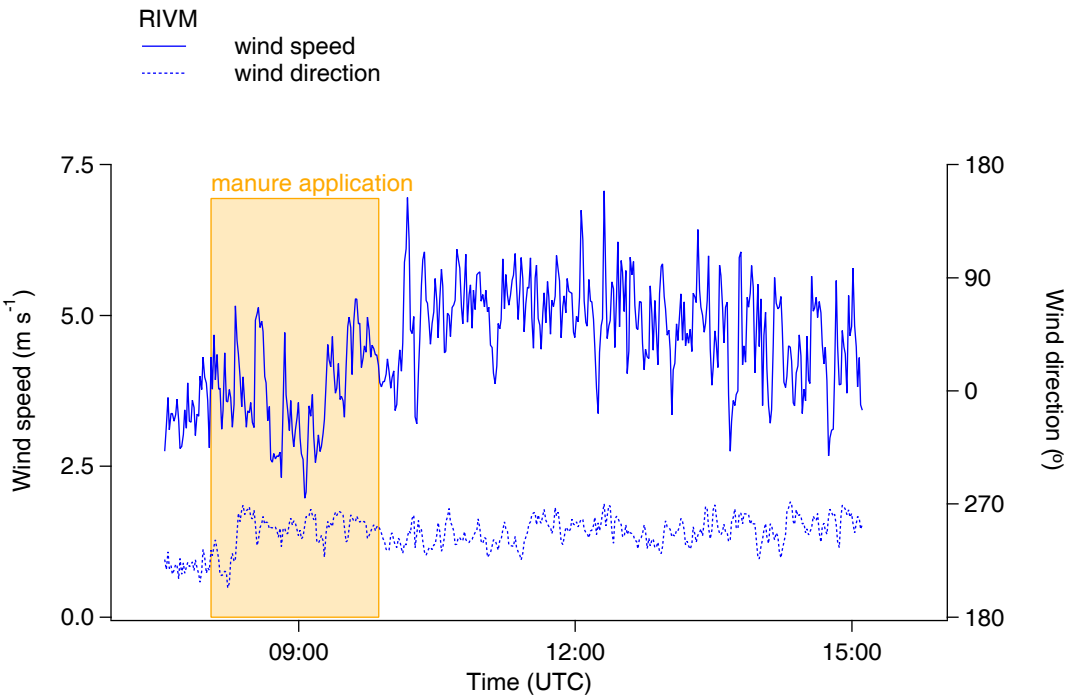

Figure 3-41. Woerden, wind speed and wind direction on 13 August 2007.

Concentration and emission measurements

Because all previous experiments had shown that the background emission, observed before the start of the manure application, was very near to zero, it was decided not to wait with the application of the manure before the lidar was operational. This way, there would be more time to record the decline of the emission rate after the manure application.

Figure 3-42 shows the emission rate and cumulative emissions for this day. On this day, 100% TAN corresponds to 54 kg NH_3-N ha^{-1}.

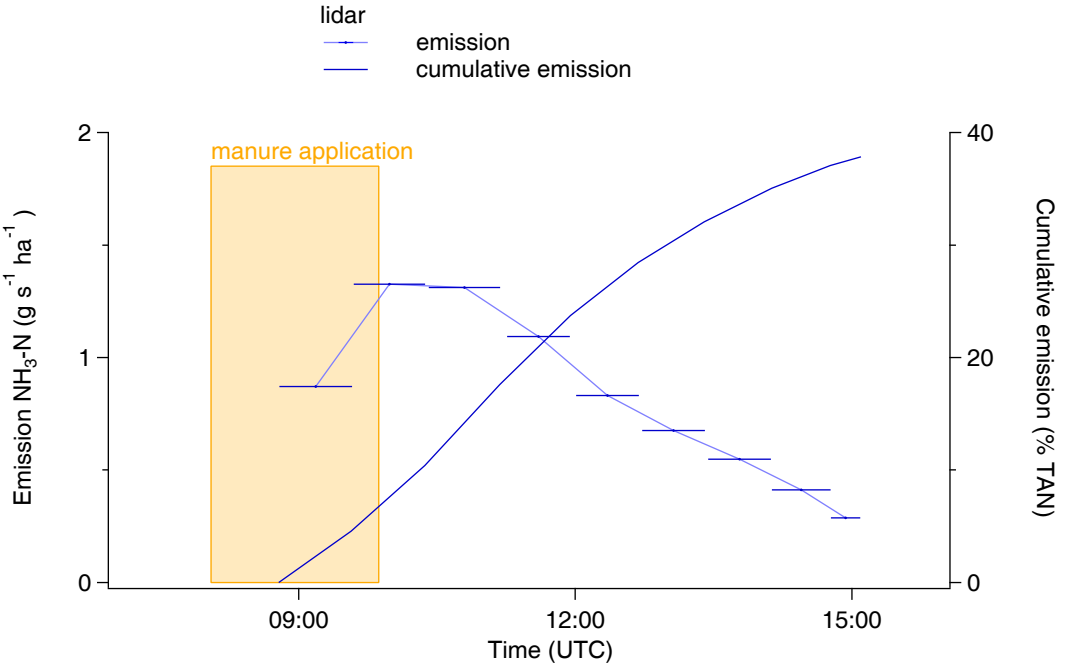

Figure 3-42. Woerden, graph showing the nitrogen emission (left axis) and the cumulative nitrogen emission (right axis) on 13 August 2007.

3.8.3 Discussion

The measured emission maximum comes about an hour after the end of the manure application. The decline in emission rate is almost linear.

3.9 General discussion

The shape of the emission rate curves agree well from one experiment day to the other. This is true for all curves from all instruments. With the exception of the second Woerden experiment (10 August 2007), all emission curves reach their maximum some two hours after manure application has ended, then start to decline. When the manure application takes some time, the ascent of the curve is gradual, rather than straight up. This leads to sigmoidal cumulative emission curves. This is unlike the modelled curves, which more resemble hyperboles.

The measured emissions were also compared to measurements performed in the past. The experiments described here lasted one or two days, while past experiments ran for four days.

- On arable land, a large variation in emission for surface spreading was observed in those past experiments. The new measurements fit within this range.
- In the experiments on grassland, about 30% of the available total ammoniacal nitrogen (TAN) evaporated during the first eight hours. Based on experiments performed in the past, the percentage of TAN expected to have evaporated after 96 hours was estimated to be on average 26% (Huijsmans

and Vermeulen 2008). These figures cannot be compared directly, since the estimates are based on an ensemble of experiments under different environmental conditions, showing a large variation. However, it can be stated that the emissions found in the experiments on grassland are relatively high, but within the range of 8 to 52% measured in experiments performed in the past. During the second day, the lidar starts to report more emission than the model as well, and the mass balance method deviates further.

4 Conclusions

The two novel methods described here, TDL and lidar, demonstrated their ability to measure ammonia emissions. Complementary to the established mass balance technique, both new techniques provide the capability to measure the emission at high temporal resolution, giving an emission value every half hour or better.

A validation experiment for the new techniques using an artificial ammonia source yielded satisfactory results for the TDL. For the lidar, results were not conclusive, due to an unfavourable experimental set-up.

The new instruments were applied to measure ammonia emissions from manured fields in six field experiments (the TDL in four), three on arable land and three on grassland. For the four experiments in which both instruments had been present, the results were compared to each other. In one of the experiments, both instruments were compared to the micrometeorological mass balance method, an established technique. In all cases, all methods showed similar emission patterns during the experiments.

Two of the experiments spanned two consecutive days. In both cases, while the largest emission was found on the first day of the experiment, a significant emission was observed on the second day as well. This emission amounted to 25% of the emission measured during the first day.

The measured emissions were also compared to measurements performed in the past. The experiments described here lasted one or two days, while past experiments ran for four days.

- On arable land, a large variation in emission for surface spreading was observed in those past experiments. The new measurements fit within this range.
- In the experiments on grassland, about 30% of the available total ammoniacal nitrogen (TAN) evaporated during the first eight hours. Based on the past experiments, the percentage of TAN expected to have evaporated after 96 hours was estimated to be on average 26%. These figures cannot be compared directly, since the estimates are based on an ensemble of experiments under different environmental conditions, showing a large variation. However, it can be stated that the emissions found in the experiments on grassland are relatively high, but within the range of 8 to 52% measured in experiments performed in the past.

In all experiments described in this report, the measured emission rates peaked around one or two hours after the end of the manure application. This was not expected; so far, in the literature an exponential decay of the emission was assumed, starting directly after application.

4.1 Recommendations

It is recommended to perform a second validation experiment with the artificial ammonia source. This is especially important for the lidar, as the experiment conducted in August 2006 was not conclusive for this method.

The greatest differences between the emissions measured with TDL or lidar and emissions measured in the past occurred on grassland. Therefore, it is recommended to focus future experiments on that type of land. The established micrometeorological mass balance method should be included in the experiments.

Additional experiments on both grassland and arable land are recommended to gain additional insight in the dynamics of the emission process. The TDL and lidar methods, with their high temporal resolution, are especially suited for such research.

It is recommended to model the process of ammonia emission, and to integrate this model with a statistical model of field measurements of ammonia losses. In this model, attention should be paid to weather conditions and manure application performance, on grassland as well as on arable land.

References

Denmead, O.T. (1983). Micrometeorological methods for measuring gaseous losses of nitrogen in the field. In: Gaseous Loss of Nitrogen from Plant-Soil Systems. J. R. Freney and J. R. Simpson (Eds.). Dordrecht, Kluwer Academic Publishers.

Force, A.P., Killinger, D.K., DeFeo, W.E. and Menyuk, N. (1985). Laser remote sensing of atmospheric ammonia using a CO_2 lidar system. Applied Optics 24 (17): 2837-2841.

Gimmestad, G.G. (2005). Differential-Absorption Lidar for Ozone and Industrial Emissions. In: Lidar: Range-Resolved Optical Remote Sensing of the Atmosphere. C. Weitkamp (Ed.). New York, Springer. 102: 187-212.

Hensen, A., Kraai, A., Van het Veen, W.H., Blom, M., Van den Bulk, W.C.M. and Bleeker, A. (2008). NH_3 emission measurements from manured fields using a mobile TDL. Petten, ECN-report in preparation.

Huijsmans, J.F.M., Hol, J.M.G. and Hendriks, M.M.W.B. (2001). Effect of application technique, manure characteristics, weather and field conditions on ammonia volatilization from manure applied to grassland. Netherlands Journal of Agricultural Science 49: 323-342.

Huijsmans, J.F.M. (2003). Manure application and ammonia volatilization. Wageningen, Ph D thesis, Wageningen Universiteit.

Huijsmans, J.F.M. and Vermeulen, G.D. (2008). Emissiefactoren uitrijden dierlijke mest. Wageningen, Wageningen UR, PRI-report in preparation.

Milieu- en Natuurcompendium, MNP, Bilthoven, CBS, Voorburg, and WUR, Wageningen. Ammoniakemissie door de land- en tuinbouw, 1990-2007 (v08, 03-09-2008). Accessed 17-09-2008, from http://www.milieuennatuurcompendium.nl/indicatoren/nl0101-Ammoniakemissie-door-de-land--en-tuinbouw.html?i=11-60.

Pasquill, F. (1974). Atmospheric diffusion: the dispersion of windborne material from industrial and other sources. 2nd Edition. Chichester, Horwood.

Van Pul, A., Van Jaarsveld, H., Van der Meulen, T. and Velders, G. (2004). Ammonia concentrations in the Netherlands: spatially detailed measurements and model calculations. Atmospheric Environment 38: 4045-4055.

Ryden, J.C. and McNeill, J.E. (1984). Application of the micrometeorological mass balance method to the determination of ammonia loss from a grazed sward. Journal of the Science of Food and Agriculture 35: 1297-1310.

Smits, M., Van Jaarsveld, H., Mokveld, L., Vellinga, O., Stolk, K., Van der Hoek, K. and Van Pul, A. (2005). VELD-project: a detailed inventarisation of ammonia emissions and concentrations in an agricultural area. Bilthoven, RIVM-report 500033002.

Stull, R.B. (1988). An Introduction to Boundary Layer Meteorolgy. Dordrecht, Kluwer Academic Publishers.

Zhao, Y., Brewer, W.A., Eberhard, W.L. and Alvarez, R.J. (2002). Lidar measurement of ammonia concentrations and fluxes in a plume from a point source. Journal of Atmospheric and Oceanic Technology 19 (12): 1928-1938.

Appendix

Potential effect of deposition on the emission determined with the TDL

Part of the ammonia emitted from the field in the experiment at the Oostwaardhoeve on 18 October 2006 will be lost due to deposition onto the 60 m strip of field that lies in between the manured circle and the measurement transect. This effect will have a maximum at the start of the experiment with the highest NH_3 concentrations passing over a field with a low-N status.

Using the Gaussian dispersion model, concentrations of NH_3 downwind of a 0.3 g s^{-1} NH_3 source were calculated on a 5 x 10 m grid. Subsequently, the concentration grid was calculated that takes into account the amount of NH_3 that would be lost due to deposition on strips of 0-10 m in the wind direction. This amount is subtracted from the initial source strength (source depletion) and a new concentration is calculated for the next strip (10-20 m) downwind of the source. This procedure is repeated for each strip up to 70 m downwind of the source. Concentrations were calculated at 0.2 m height and deposition was calculated using these concentration levels in combination with a deposition velocity of 0.016 m s^{-1}. The calculation suggests a removal of about 10% of the emitted NH_3 in the 60 m area downwind of the source.

Table 4-1. Initial run of the Gaussian model.

distance (m)	10	20	30	40	50	60	70
-50	0	0	0	0	0	0	0
-45	0	0	0	0	0	0	0
-40	0	0	0	0	0	0	0
-35	0	0	0	0	0	0	1
-30	0	0	0	1	2	5	9
-25	0	3	9	18	29	40	50
-20	62	109	143	162	172	177	177
-15	1973	1015	750	610	519	452	402
-10	3380	2112	1423	1074	859	713	608
-5	2585	2066	1429	1115	917	777	672
0	2196	1662	1167	938	795	692	612
5	1837	1440	998	789	660	571	505
10	1713	1095	763	596	493	423	372
15	987	509	378	312	270	241	219
20	31	55	71	81	87	90	92
25	0	1	4	9	15	20	25
30	0	0	0	0	1	3	4
35	0	0	0	0	0	0	0
40	0	0	0	0	0	0	0
45	0	0	0	0	0	0	0
50	0	0	0	0	0	0	0

Figure 4-1 shows the initial with concentration levels close to the source that were in the same order of magnitude as observed with the lidar. At 60 m distance, the concentrations observed with the mobile measurement system were below the model estimate (up to 400 instead of 600 µg m^{-3}).

The concentration patterns in the centre of the plume, both for the initial run and for the run that included deposition, are shown in Figure 4-1. The concentration level is about 10% lower due to the deposition. When it is assumed that this also accounts for the concentration level at 2.7 m height, concentration peaks of about 500 µg m^{-3} would be observed. At 60 m, plume dispersion accounts for 70% of the concentration decrease (from 2300 to 690 µg m^{-3}), deposition enlarges the decrease by only a fraction: 73% (from 2300 to 621 µg m^{-3}).

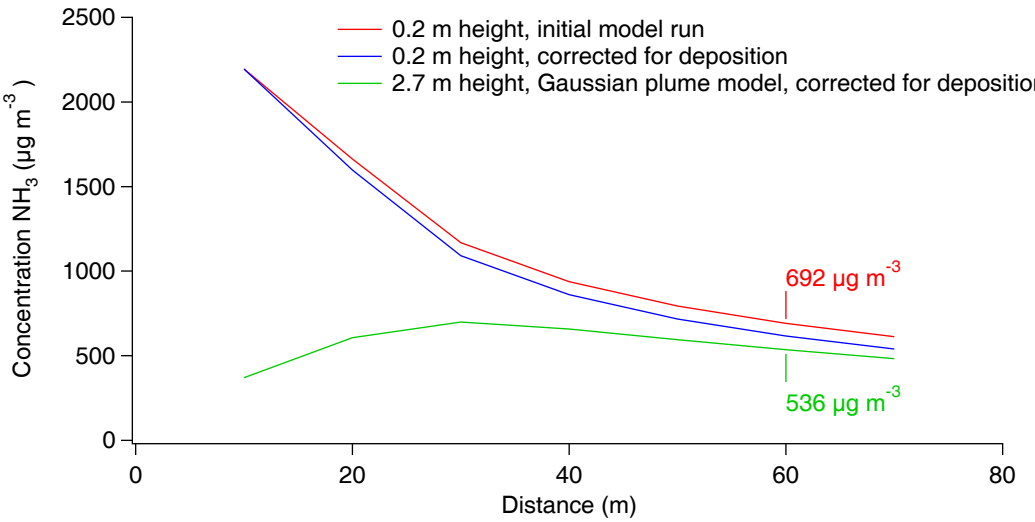

Figure 4-1. Concentration on the plume axis for various model runs.

RIVM

National Institute
for Public Health
and the Environment

Laboratory for Environmental
Monitoring

P.O. Box 1
3720 BA Bilthoven
the Netherlands
www.rivm.nl